Synthesis and Evaluation of Indole Cyanoacrylic Acids as Anticancer Agents

A THESIS

SUBMITTED TO THE FACULTY OF

UNIVERSITY OF MINNESOTA

BY

KEBREAB SAMUEL

IN PARTIAL FULFILLMENT OF THE REQUIREMENTS

FOR THE DEGREE OF

MASTER OF SCIENCE

Dr. Joseph L. Johnson

DECEMBER 2016

ACKNOWLEDGEMENTS

I would like to thank my advisors Dr. Joseph Johnson and Dr. Venkatram Mereddy for their valuable effort, time, and energy through my graduate school career. I am grateful to my advisors for their support, encouragement and patience. I would also like to thank my committee member Dr. Paul Siders for devoting his valuable time and support.

I am grateful to my colleagues Sravan Jonnalagadda, Lucas Solano, Shirisha Gurrapu, Conor Ronayne, Grady Nelson and Min Kyung Sohn. Especially, I am greatly indebted to Shirisha for all her valuable input in writing this paper.

It is a pleasure to thank the department of Chemistry and Biochemistry of University of Minnesota Duluth for giving me the opportunity of a lifetime to further my education. I would equally like to express my gratitude to all faculty members of the chemistry department.

Finally, I would like to thank my dearest wife Lul, my parents Rediet and Hadas, and all my family members including Rebecca, Moses and Martha for making my dream come true through their continuous love and support in every step of my life.

ABSTRACT

Cancer is the second leading cause of death in the United States. Breast cancer is common among women, and triple negative breast cancer accounts 10-20% of all breast cancer patients. Cancer has seemingly unlimited proliferative capacity and can spread easily to other parts of the body, making it difficult to treat. Cancer cells meet their high-energy requirement by changing their metabolic pathway in a process called "Warburg effect" via increased glycolysis independent of the presence or absence of oxygen. The increased glycolysis, which fuels hypoxic cancer cells for their high-energy demand, produces lactate. Transport of lactate and pyruvate through the plasma membrane is mediated by a group of integral membrane transport proteins, which are called monocarboxylate transporters (MCTs). Inhibition of MCT results in the starvation of tumor cells and, eventually, leads to their death. Therefore targeting MCTs could be an effective way to reduce aggressive spread of cancer in the body. In this thesis, a library of indole based small molecules have been synthesized and characterized. Furthermore their MCT1 inhibition has been evaluated in RBE4 cell line. It was found that most of the indole cyanoacrylic acids exhibited good MCT1 inhibition while compounds **1**, **11-13** didn't show any activity. Based on their good MCT1 inhibition, compounds **9** and **10** were selected as the lead candidate compounds. Future studies will include the evaluation of the lead candidates for their systemic toxicity, and *in vivo* anticancer efficacy in tumor xenograft models.

TABLE OF CONTENTS

LIST OF SCHEMES

LIST OF FIGURES

LIST OF TABLES

LIST OF ABBREVIATIONS

ATP	adenosine triphosphate
bFGF	Fibroblast growth factor-basic
CHC	α-cyano-4-hydroxycinnamate
CH_2Cl_2 (DCM)	methylene chloride (dichloromethane)
CH_3CN	acetonitrile
DMAP	4-N,N-dimethylaminopyridine
DMF	N,N-dimethylformamide
DMSO	dimethyl sulfoxide
ECM	extracellular matrix
EGFR	epidermal growth factor receptor
EPO	erythropoietin
Et_3N	triethylamine
EtOAc	ethylacetate
FDG	fluorodeoxyglucose
GLUT	glucose transporters

HBTU	2-(1*H*-benzotriazol-1-yl)-1,1,3,3-tetramethyluronium hexafluorophosphate
$HCOONH_4$	ammonium formate
HER2	human epidermal growth factor receptor 2
HIF-1	hypoxia-inducible factor 1
K_2CO_3	potassium carbonate
MCTs	monocarboxylate transporters
OxPhos	oxidative phosphorylation
Pd/C	Palladium on charcoal
PET	positron emission tomography
$POCl_3$	phosphoryl chloride
TAT1	T-type amino-corrosive transporter-1
THF	tetrahydofuran
TNBC	triple negative breast cancer
VEGF	vascular endothelial growth factor

CHAPTER 1: INTRODUCTION

For a body to function normally, cells have to grow, divide and die. These processes happen in a controlled fashion. Sometimes, cells undergo uncontrolled growth and interfere with normal functioning of the body by reaching a critical mass or by spreading to another location via metastasis. This abnormal growth eventually leads to the death of the individual. This condition is called “cancer”.

Hallmarks of cancer: A focus on tumor metabolism

Many cancers have some common underlying features, but they also possess unique pathologies and differences in their metabolic processes. An increased dependency on glycolysis for ATP production is considered to be one of the important hallmarks of tumor cells.[1-2] Understanding and targeting these hallmarks of cancer is broadly accepted as a promising strategy for therapeutic intervention to prevent, treat and eliminate cancer and provides a set of very attractive targets to guide the design of new drugs.[1-2] The following are some of the crucial hallmarks of cancer that can be targeted to develop new treatments for cancer (**Figure 1**).

Figure 1: Hallmarks of cancer: Acquired capabilities (Modified from ref 1)

Acquired growth signal independence or self-sufficiency: Normal cells need growth signals to undergo proliferation from a quiescent state, and they do not undergo proliferation without these stimulatory signals. However, tumor cells do not depend on external growth stimulation. Three common strategies through which cancer cells become independent of outside growth signals are: a) changing of extracellular growth signals; b) transcellular transduction of those signals; and c) intracellular circuits that translate those signals into action. A cancer cell is capable of making its own growth factors to facilitate its proliferation and becomes independent of other cells. The cell surface receptors that transduce growth stimulatory signals into the cell interior become unregulated during the progression of the tumor. Vascular endothelial growth factor

(VEGF), epidermal growth factor receptor (EGFR), and human epidermal growth factor receptor 2 (HER2) are some of the examples of induced growth signal transduction.[1-2]

Insensitivity to anti-growth signals: Anti-growth signals control the proliferation of normal cells by forcing them to enter in to quiescent state and also reduces their growth potential by inducing them into a post mitotic state. However, cancer cells develop strategies to bypass the antigrowth signals and divide uncontrollably.[1-2]

Evading apoptosis: Apoptosis is a programmed cell death which is a critical process for the survival of multicellular organisms. Cancer cells bypass it to grow and divide uncontrollably by avoiding cellular death pathways. p53 is a cancer suppressor gene and a major part of the DNA damage sensor that can instigate the apoptotic cascade. When p53 is mutated or missing, cancer cells evade apoptosis. Cancer cells are also known to weaken the activity of p53 by inhibiting it and silencing its activators.[1-2]

Limitless replicative potential: Normal cells are able to keep track of the number of their cell divisions. Usually after 40-60 divisions, cell growth slows down and eventually stops. This state, known as senescence, is irreversible. Cancer cells generally deviate from a normal cellular growth program and breach the limit of replication and divide endlessly.[1-2]

Sustained angiogenesis: Angiogenesis is a coordinated growth of new blood vessels from pre-existing blood vessels. Tumors are limited in their growth beyond a certain size due

to the lack of oxygen and access to other essential nutrients. Tumors induce blood vessel formation by secreting growth factors such as fibroblast growth factor-basic (bFGF) and VEGF that initiate capillary growth into the tumor, which in turn allows for tumor expansion by supplying nutrients.[1-2]

Tissue invasion and metastasis: Tumors are surrounded by extracellular matrix (ECM). After a certain stage, tumors cannot grow and hence it is possible for a few tumor cells to evade the contact with the ECM, escape, and be transported to new areas of the body such as brain, lungs, liver, bones, etc. These new regions have the nutrients to support the growth of the metastasized tumor cells to form secondary tumors.[1-2]

Warburg effect in cancer cells

Generally, in normal cells, oxidative phosphorylation (OxPhos) of pyruvate to CO_2 and H_2O takes place in the mitochondria to generate energy in the form of ATP. Similarly, cancer cells must also produce energy that can allow them to proliferate. Tumor cells often alter their metabolic pathways to bypass the checkpoints in cell division. Some of the changes in metabolic pathways serve to shift the generation of ATP from OxPhos to glycolysis.[3-9] Glucose metabolism in cancer cells is essentially distinguished by two principal biochemical phenomena: an increased glucose uptake and increased levels of glycolysis. Glycolysis encompasses the conversion of glucose to pyruvate and lactate. Under aerobic conditions, glycolysis typically favors the production of pyruvate, which then feeds into the OxPhos pathway where ATP production is coupled with the reduction of O_2 to H_2O. Conversely, glycolysis under anaerobic cellular conditions typically favors the formation of lactate as the terminal step of glycolysis. In cancer cells, glycolysis is the preferred source of ATP production even in the presence of oxygen, a process termed as "Warburg effect" (**Figure 2**).[3-9] Cancer cells require significant amount of glucose for their rapid proliferation. Adaptation of glycolysis is a survival mechanism for all advanced stage tumors and starving the cancer cell of necessary energetic requirement for rapid and uncontrolled proliferation can inhibit glycolysis. Thus, inhibition of glycolysis can be a useful target for the development of anticancer agents for cancer treatment.[10-11]

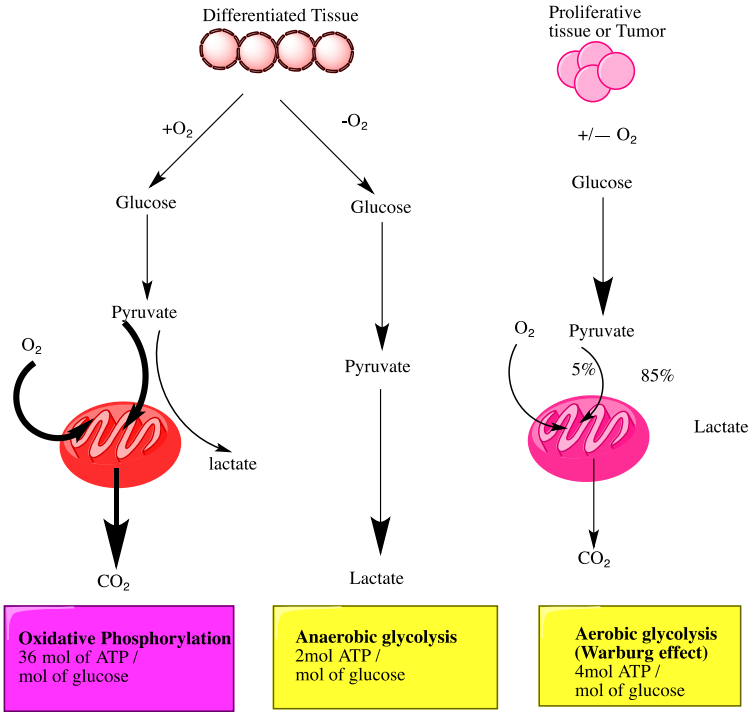

Figure 2: Glucose metabolism in normal and cancer cells

The elevated glucose requirement of cancer cells compared to normal cells is applied in ^{18}F fluorodeoxyglucose (FDG, **Figure 3**) based positron emission tomography (PET). FDG-PET is a screening method used in distinguishing malignant cancer cells from normal cells by quantitatively analyzing glucose metabolism. As stated before, malignant cancers have high rate of glucose metabolism.[12-13]

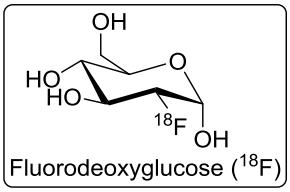

Figure 3: Fluorodeoxyglucose (^{18}F)

Tumor hypoxia:

Tumor cells require excessive nutrients to proliferate continuously and, hence, they develop new blood vessels to meet energy requirements. As the tumor continues to grow, some regions of tumor are deprived of oxygen and this condition is called "hypoxia". Hypoxia is a common characteristic of numerous solid tumors. The adjustment of cancer cells to hypoxic conditions is mediated by hypoxia-inducible factor 1 (HIF-1), which is a major transcription factor involved in upregulating a series of genes including VEGF, angiogenesis, erythropoietin (EPO), glucose transporters (GLUT), and several glycolytic enzymes involved in glucose metabolism. Hypoxia-induced gene expression in cancer cells has been correlated with malignant transformation. However, studies suggest that lactate and pyruvate have the ability to direct hypoxia-inducible gene expression without the need for hypoxic conditions by expressing HIF-1α. Tumor hypoxia also correlates with treatment failure, relapse and, patient mortality as these cells are generally resistant to standard chemo- and radiation therapies.[14-16]

Monocarboxylate transporters (MCTs):

In hypoxic cells, metabolism of glucose to lactate generates only 2 ATPs per molecule of glucose whereas oxidative phosphorylation generates up to 36 ATPs. Therefore, in order to overcome this inefficient energy production, tumor cells have to consume large amounts of glucose at a rapid pace to fuel the hypoxic cells and produce lactate.[14-16] Transport of lactate and pyruvate through the plasma membrane is catalyzed by a group of integral membrane transport proteins, which are called the

monocarboxylate transporters (MCTs).[17-20] Not only do the cancer cells consume a large amount of glucose, but they also overexpress/upregulate the related enzymes including MCT's. The MCT family is made up of 14 members, namely MCTs 1–9, MCTs 11–14 and T-type amino-corrosive transporter-1. MCTs 1-4 are involved in transporting proton-linked monocarboxylates such as lactate, pyruvate, acetoacetate and β-hydroxybutyrate through the plasma membrane. MCT8, known as SLC16A2, is a thyroid hormone transporter and MCT-10 is an aromatic amino acid transporter. The function of the other MCTs is not clearly understood.[17-20]

MCT1 consists of 494 amino acids with an atomic weight of ~53 KDa and 12 transmembrane domains. Substrate conditions and pH can significantly influence the ability of MCT1 to facilitate the movement of lactate in and out of the cell. The transporter can trade one monocarboxylate molecule for another without a net exchange of protons.[17-20] However, in other tissues like the red blood cells, white skeletal muscle, and tumor cells, it transports lactic acid out of the cell where the metabolism is highly glycolytic. This is crucial for cancer cells which primarily depend on glycolysis due to mitochondrial dysfunction and lack of ATP production via OxPhos as a result of hypoxic conditions.[14-16]

MCT4 has a molecular weight of ~43 KDa and also spans the membrane. Tissues in the human body with high expression of MCT4 are white skeletal muscle fibers astrocytes, white blood cells, chrondrocytes and tumor cells, which are known for their high glycolytic rates.[21-22] Both MCT1 and MCT4 have great similarities in terms of tissue distribution, regulation and substrate/inhibitor specificity. MCT4 has a low affinity for a

variety monocarboxylates when compared to MCT1. The K_m of MCT4 for most monocarboxylates such as pyruvate is more than 100 mM, except for L-lactate, which is about 30 mM. These lower affinities of MCT4 for different substrates compared to MCT1 was also observed for many inhibitors.[21-22] MCT4 expression is increased in cancer cells as a result of delayed hypoxia through a transcriptional regulatory component involving HIF-1α.[23] High levels of MCTs are commonly expressed in a range of human tumors, including breast, head and neck, prostrate, brain tumors.[24-32]

Stromal-epithelial metabolic coupling, and reverse Warburg effect:

Recent studies by Lisanti *et al.* on metabolic processes in epithelial cells show that the tumor microenvironment consists of stromal fibroblasts and epithelial cancer cells. These cancer cells use oxidative stress as a means to get nutrients from surrounding fibroblasts. Epithelial cancer cells initiate oxidative stress in neighboring stromal fibroblasts by releasing hydrogen peroxide resulting in mitochondrial dysfunction and increased dependence upon glycolysis and the associated increased production of lactate and pyruvate. These metabolic products are transported by MCTs to feed and proliferate adjacent epithelial cancer cells, which can generate ATP via oxidative phosphorylation. Thus, they form parasite-host relationship in which the aggressive cancer cells are parasites (**Figure 4**).[33-36]

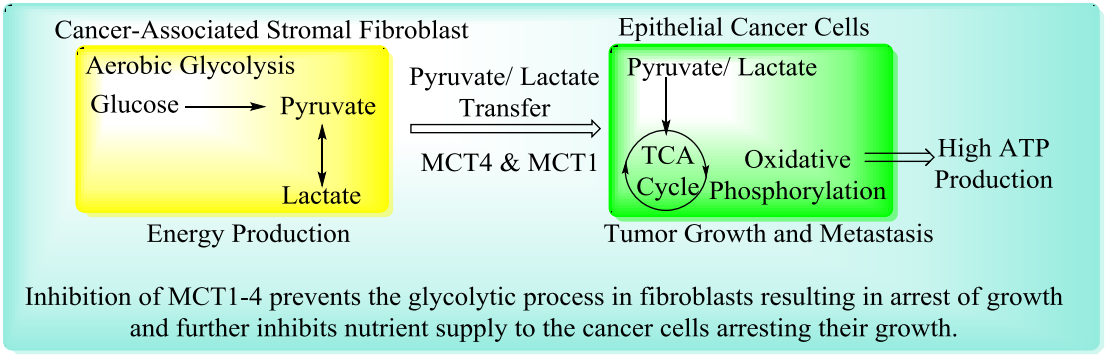

Figure 4: Stromal-epithelial metabolic coupling and reverse Warburg effect

Triple negative breast cancer

Triple negative breast cancer (TNBC) accounts for 10-20% of all breast cancers. The term triple negative is an operational term which refers to all heterogeneous breast cancers and commonly affects young women of African-American, Hispanic origins

and/or those with a BRCA1 gene mutation.[37,38] Generally, breast cancer drugs are targeted towards hormone receptor markers such as estrogen receptor (ER), progesterone receptor (PR), and human epidermal growth factor receptor 2 (HER2) for treatment. Tamoxifen and raloxifen are the drugs that target hormone receptors, whereas, herceptin is used to target HER2. The absence of well-defined biomarkers makes the treatment of TNBC more difficult. The standard treatment for TNBC includes surgery, radiation and chemotherapy with anthracyclins and taxane-based medications. The fact that these drugs are not cancer cell selective in addition to their serious side effects makes them inefficient in the treatment of cancer. Most patients initially respond to the chemotherapy but a majority relapse, and the cancer becomes drug resistant. Subsequently, novel therapeutics that are specifically harmful to tumor cells and ideally that work on drug resistant cells are highly critical.

Cancer treatment, which has long depended on the prevention of rapid proliferation of tumor cells for effective treatment, was found to be ineffective due to the undesirable side effects caused by the lack of specificity in the approach. Cancer cells shift to a dependence upon glycolytic metabolism as an adaptation mechanism to hypoxia in order to fulfill the high bioenergetic and bisosynthetic demand of proliferating cells, which also creates a lactate gradient. MCT1 and MCT4 are largely expressed in cancer cells for the transport of metabolites, and are especially upregulated in response to hypoxia. By inhibiting MCT1 or MCT4, the transport of lactate is inhibited in hypoxic regions, and the aerobic cancer cells cannot proliferate due to the lack of lactate. In addition, the pH in hypoxic cells decreases resulting in acidosis and cell death. The aerobic cells can easily be treated with chemotherapy and radiation. Therefore, targeting

both MCT4, which is a direct transcriptional target of HIF-1α, and MCT1 could hinder the transport of lactate and effectively target the tumor cells.[39, 40]

Recent studies on MCT inhibitors:

In recent years, numerous molecules have been synthesized and evaluated as MCT inhibitors. The following is a brief insight into these inhibitors.

α-Cyano-4-hydroxycinnamate (CHC, **Figure 5**) is a known MCT1 inhibitor. CHC specifically and significantly inhibits pyruvate transport in liver mitochondria and erythrocytes. The fact that it specifically inhibits pyruvate but not acetate or butyrate transport suggests that MCT1 is specifically involved in the transport of lactate across plasma membranes and across the inner membrane of mitochondria. Pyruvate transport inhibition studies by CHC were conducted using mitochondrial incubation media at very low concentrations (<200 μM) and the rate of pyruvate oxidation by mitochondria from blowfly flight muscle and rat heart was determined.[41]

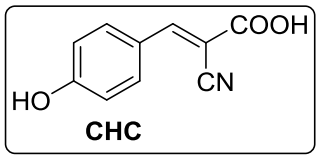

Figure 5: α-Cyano-4-hydroxycinnamate

U-87 is a well-established model for glioblastoma multiforme and show elevated MCT1 expression. CHC was evaluated for its anticancer efficacy in glioblastoma tumor xenograft model in immunodeficient rats.[42] Rats were stereotactically implanted with glioma cells and CHC was administered via osmotic pump for the treatment. MRI images

were obtained for the treated and untreated rats. The tumor burden was significantly decreased in rats that received treatment with CHC on day-120 whereas in the untreated group, tumor size increased by day-20. This clearly suggests that CHC inhibits MCT1 in glioblastoma tumor model.

In another study, a Lewis lung carcinoma tumor xenograft model, which also overexpresses MCT1, was treated with CHC (MCT1 inhibitor) and the tumor growth was slowed over an 8 day period compared to the vehicle group.[16]

AZD3965, an MCT1 inhibitor, was also implicated in the radiosensitzation of small cell lung carcinoma (SCLC) model.[43] Immunocompromised CD-1 mice were inoculated with H526 cells and mice were treated with 100 mg/kg of AZD3965 compound for three days, followed by the treatment with 2Gy radiation. The mice were monitored for an additional period of time until the tumor volumes reached 1000 mm^3. Treated groups showed a took an additional 4 days to reach 1000 mm^3 (12 days) compared to the group treated with radiation only, which took 8 days.

Based on the above studies, MCT inhibition leads to a decrease in tumor growth and can radiosensitize the tumor cells and improves the survival of rodent tumor xenograft models. Hence, MCT is an extremely important glycolytic target to treat advanced stage tumors. In connection with the above statement, many CHC derivatives have been synthesized in recent years with good *in vitro* MCT1 inhibition and *in vivo* efficacy.[44]

In cyanocinnamate compounds, the substitution of the OH group on the benzene ring by the N,N-dialkyl groups lead to an exponential increase in activity (**Figure 6**). These compounds showed better IC_{50} values while maintaining great MCT1 inhibitory potency compared to CHC. Above all, the easiness of their synthesis, water solubility and non-toxicity to other cells makes them very desirable and opens the way for further research and synthesis of other cyanocinnamate derived compounds.[44]

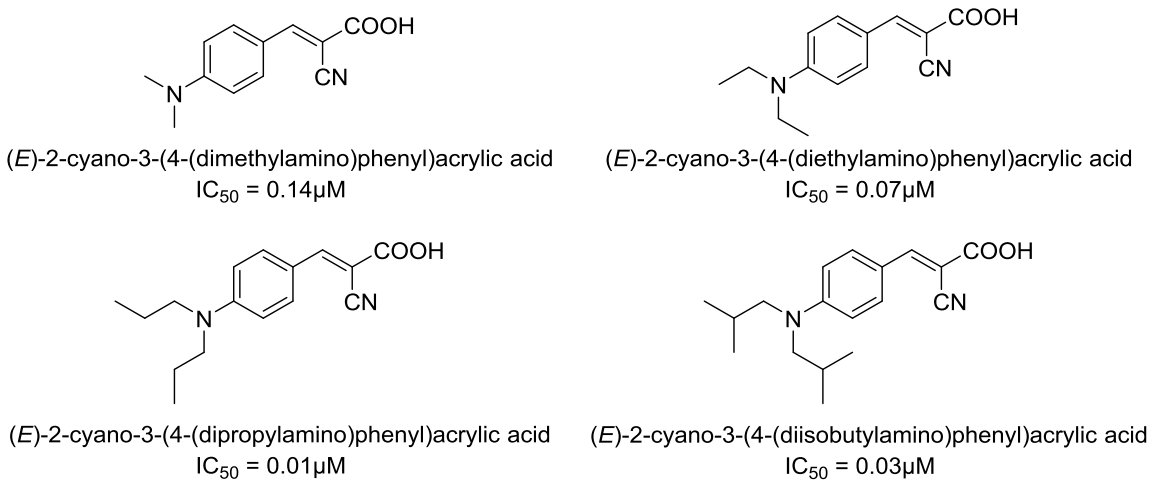

Figure 6: Examples of CHC derived compounds with MCT1 IC_{50} values

Therefore this project was designed on the hypothesis that synthesis and biological evaluation of compounds which have both the indole moiety and cyanocinnamic acid unit could achieve better anti proliferative and MCT1 inhibitory potency. In this regard, we have synthesized novel indole based cyanocinnamate derivatives and evaluated them for their MCT1 inhibition.

Indole is a pharmacologically privileged chemical structure and many indole-

based pharmaceuticals are in the clinical usage for the treatment of various diseases. Hence, we envisioned to synthesize several indole based compounds as potential MCT and tumor metabolism inhibitors.

The indole moiety is a critical pharmacological unit that is found in essential amino acid tryptophan, neurotransmitter tryptamine, serotonin, melatonin, etc. (**Figure 7**).[45-47]

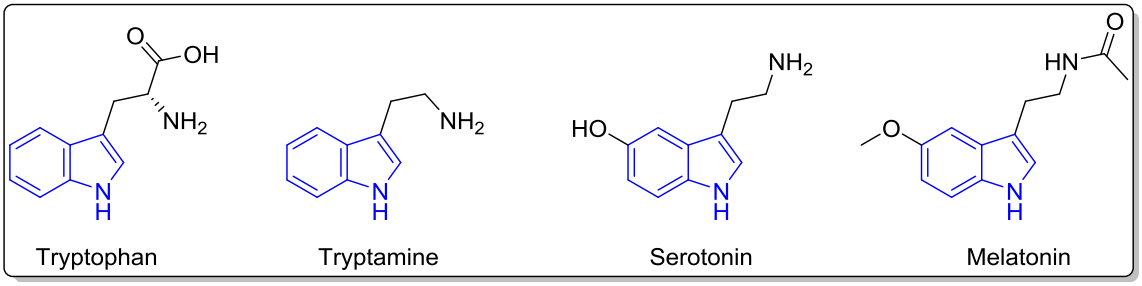

Figure 7: Important indole containing molecules

Indole is also an important pharmacophore in clinically used drugs such as 5-THS3 antagonist alosetron for the treatment of irritable bowel syndrome in women, indomethacin used for rheumatoid arthritis, sumatriptan for migraine management, ondansetron which is used as an antiemetic to control nausea and vomiting in patients who undergo chemotherapy for cancer treatment (**Figure 8**).[48]

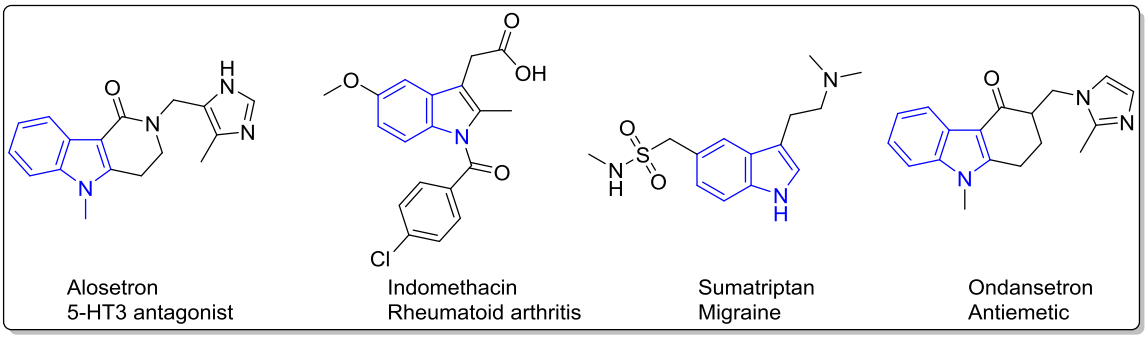

Figure 8: Clinically used indole molecules

CHAPTER 2: RESULTS AND DISCUSSION

As mentioned above, indole based compounds are pharmacologically and pharmaceutically privileged nitrogen-containing heterobicyclic compounds. These compounds are responsible for a variety of biological activities and sometimes mimic endogenous substrates by binding to proteins. In fact, indole is the core of the amino acid tryptophan and other important derivatives such as melatonin and serotonin. Hence, indole has a vital role in the central nervous system.

Hypothesis and purpose of the work

Owing to the great success of indole based pharmaceuticals in clinic, we hypothesized that indolyl cyanoacrylates would be excellent compounds for the inhibition of MCT function. We envisioned that if these novel compounds exhibited potent MCT1 or MCT4 inhibition or cytotoxicity, they could be developed as potential tumor glycolysis inhibitors. The main purpose of this project is to synthesize and explore indolyl cyanoacrylates as anticancer agents with potential mechanisms in the disruption of tumor glycolysis and other metabolic pathways.

Synthesis of (E)-2-cyano-3-(1H-indol-3-yl)acrylic acid

(E)-2-cyano-3-(1H-indol-3-yl)acrylic acid **3** was synthesized using indole as a starting material. 1H-indole **1** was formylated using Vilsmeier Haack condition to obtain 1H-indole-3-carbaldehyde **2**. This product **2** was further reacted with cyanoacetic acid via Knoevenagel condensation to get indole cyanoacrylic acid **3** in 69% yield (**Scheme 1**).

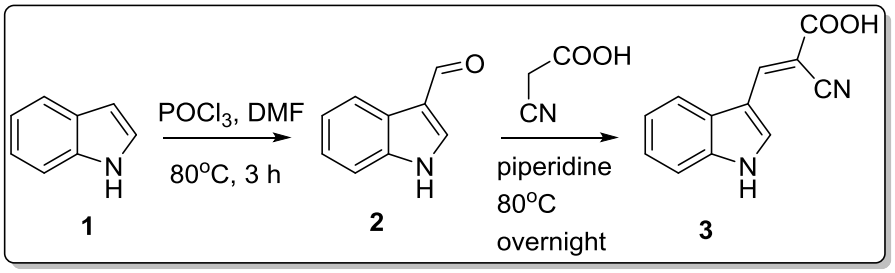

Scheme 1: Synthesis of (E)-2-cyano-3-(1H-indol-3-yl)acrylic acid

Synthesis of (E)-2-cyano-3-(1-(4-substituted benzyl)-1H-indol-3-yl)acrylic acids

1-(4-substituted benzyl)-1H-indole cyanoacrylic acids **4-8** were synthesized starting from 1H-indole **1** and substituted benzyl bromides. We have utilized benzyl bromide, 4-ethylbenzyl bromide, 4-methoxybenzyl bromide, 4-chlorobenzyl bromide and 4-bromobenzyl bromide. First, benzyl bromides were prepared by reducing substituted benzaldehyde with sodium borohydride and subsequent bromination of alcohol with PBr_3. Then, **1** was alkylated using these corresponding bromides followed by Vilsmeier Haack formylation and Knoevenagel condensation to obtain (E)-2-cyano-3-(1-(4-substituted benzyl)-1H-indol-3-yl)acrylic acids in 50-70% yields (**Scheme 2**).

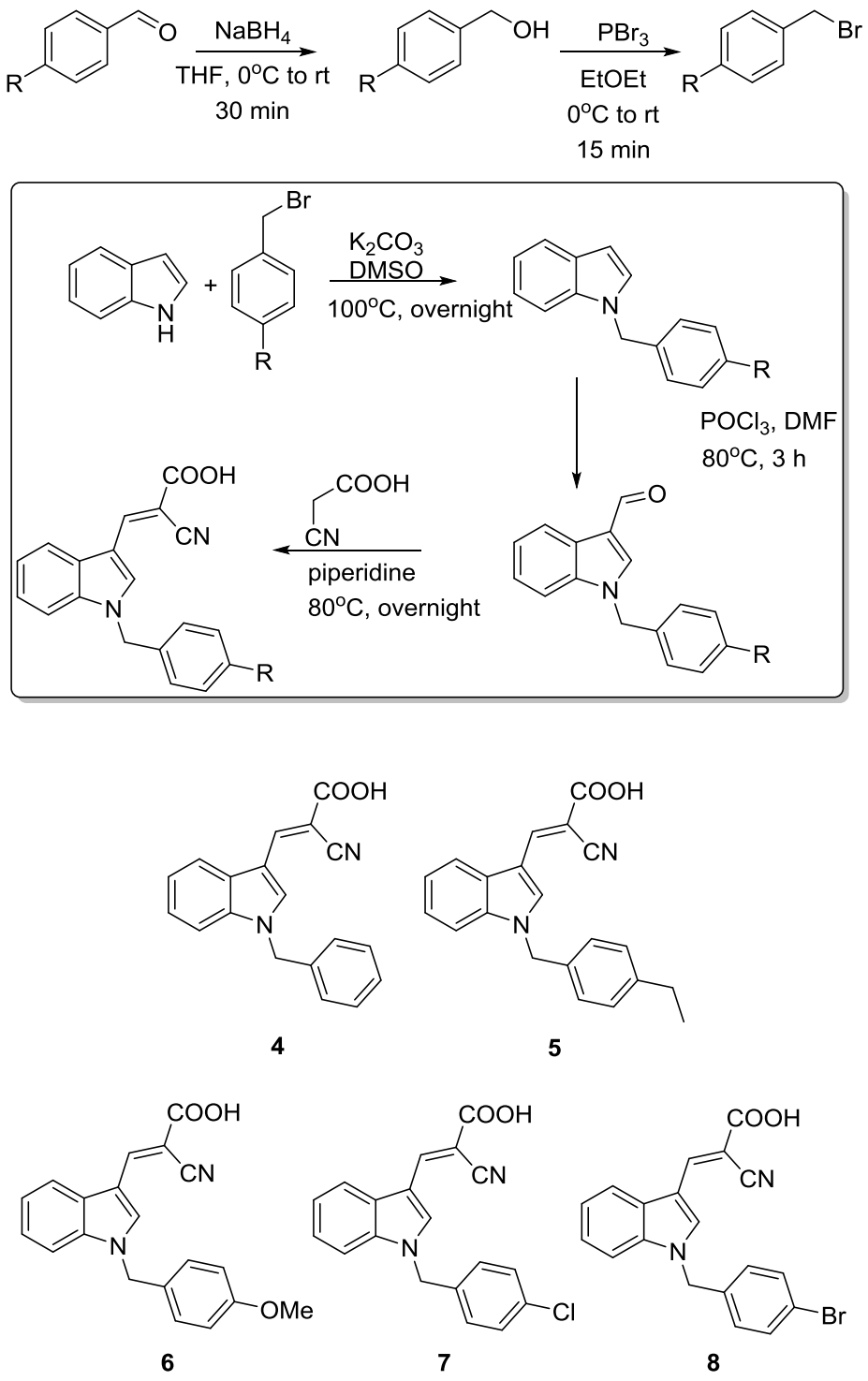

Scheme 2: Synthesis of (E)-2-cyano-3-(1-(4-substitutedbenzyl)-1H-indol-3-yl)acrylic acids

Synthesis of (E)-2-cyano-3-(1-(4-substituted phenyl)-1H-indol-3-yl)acrylic acids

(E)-2-cyano-3-(1-(4-substituted phenyl)-1H-indol-3-yl)acrylic acids **9-13** were synthesized starting from 1H-indole **1** and 1-iodo-4-substituted benzenes. We utilized simple iodobenzene, 1-iodo-4-methoxybenzene, 2-bromopyridine, 3-bromopyridine and 2-iodobenzoic acid. Here, **1** was reacted with 1-iodo-4-substituted benzene in presence of K_2CO_3, CuI, L-proline to obtain 1-(4-substituted phenyl)-1H-indole, which was converted to aldehyde and condensed to cyanoacrylic acids **9-13** (50-78% yield) using Vilsmeier Haack formylation and Knoevenagel condensation, respectively (**Scheme 3**).

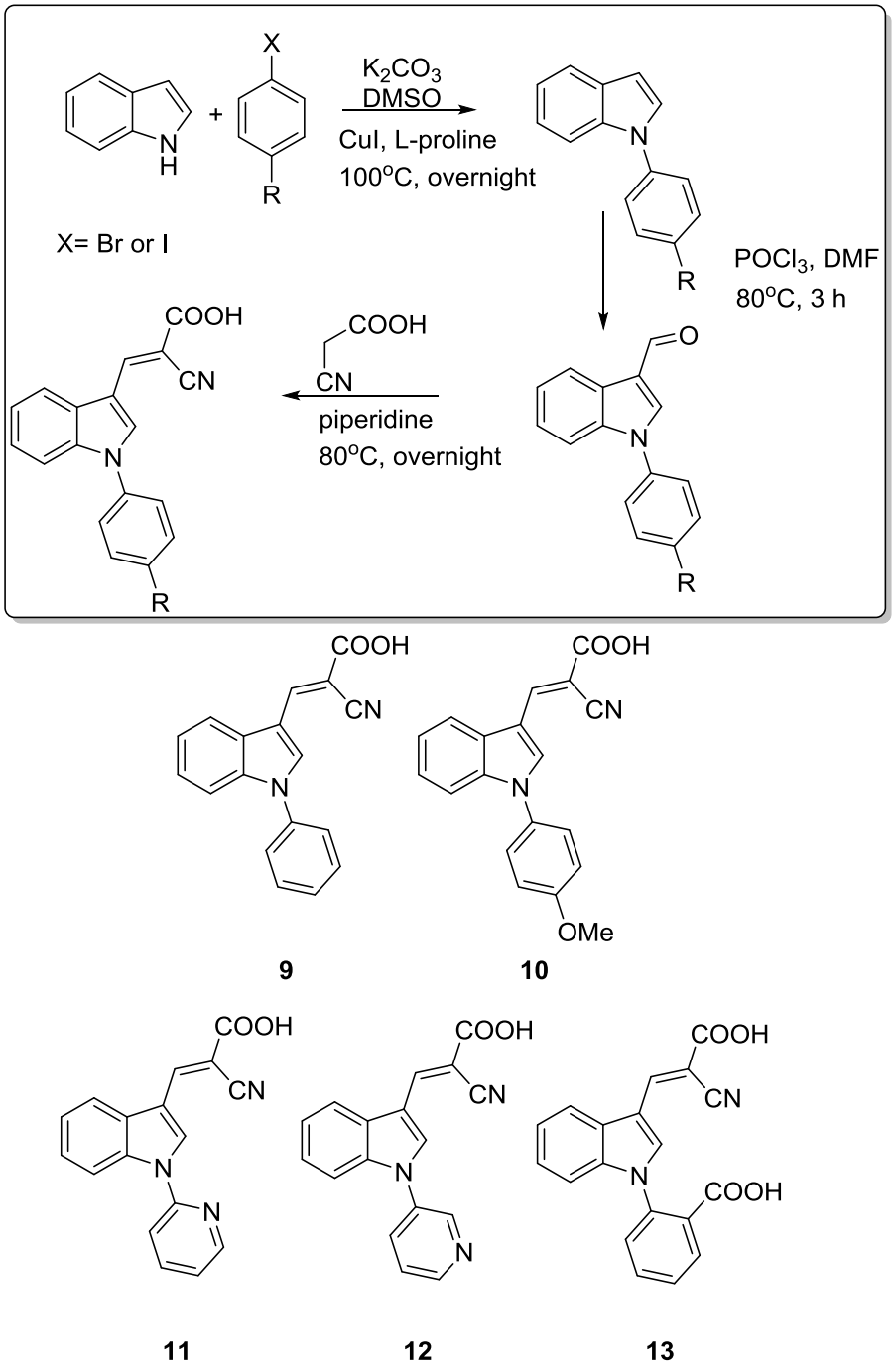

Scheme 3: Synthesis of (E)-2-cyano-3-(1-(4-substituted phenyl)-1H-indol-3-yl)acrylic acids

Biological Evaluation

To evaluate the biological activity of indole cyanoacrylic acids, we carried out MCT1 inhibition assay on rat brain endothelial 4 (RBE4) cell line using sodium salt of [^{14}C]-L-lactic acid. RBE4 is a non-cancerous cell line with high MCT1 expression.[44]

Approximately 2x10^5 cells/well were plated in 24-well plate and incubated in 5% CO_2 atmosphere for 16 -24 hours. The cells were washed with HEPES buffer. The buffer was removed and test compounds in [^{14}C]-L-lactate solution were added for influx of lactate for 15 minutes. The test compounds were removed and stop buffer was added and kept on ice. The cells were then lysed with 0.1 M triton-X Solution. Uptake values of the lysed cells were obtained in dpm (disintegrations per minute) using Scintillation counter.

Table 1: IC_{50}* (nM) values of indole derivatives for MCT1 inhibition

Compound No.	Compound	MCT1 IC_{50}
3	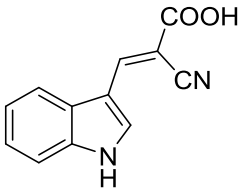	>1000
4	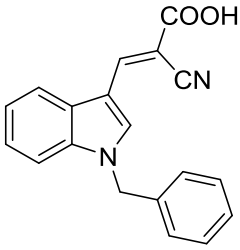	65.9±10.9

5	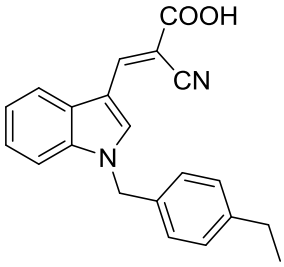	36.3±14.1
6	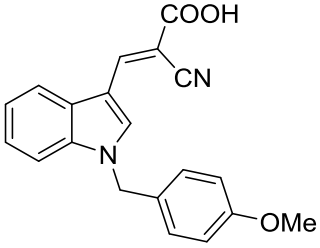	107.0±10.5
9	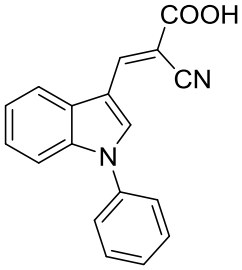	12.8±2.6
10	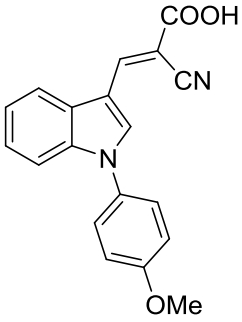	21.9±2.9
11	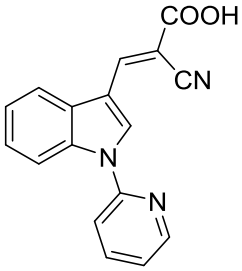	>1000

12	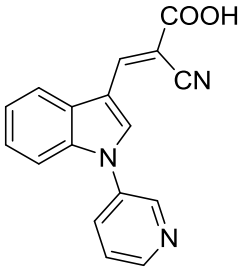	>1000
13	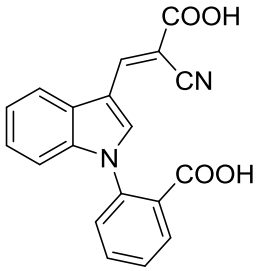	>1000

*IC_{50} is expressed in avg±SEM nM, average of minimum 3 experimental values

Based on the interesting biological results obtained for indole cyanoacrylic acids, we also prepared indole benzamido cyanoacrylic acids **21** and **22** with a phenyl spacer between amide and indole groups.

Synthesis of N-(4-(1H-indol-1-yl)phenyl)benzamide:

Indolyl amide **15** was synthesized using indole as a starting material. The first step involved nucleophilic ipso substitution of 1H-indole **1** by 4-fluoro nitrobenzene under basic conditions to obtain 1-(4-nitrophenyl)-1H-indole **16**. The nitro group was further reduced using ammonium formate and palladium-carbon to obtain the corresponding amine **17**. Benzoylation of the indole amine using benzoyl chloride resulted in the formation of indolyl amide **18** (**Scheme 4**).

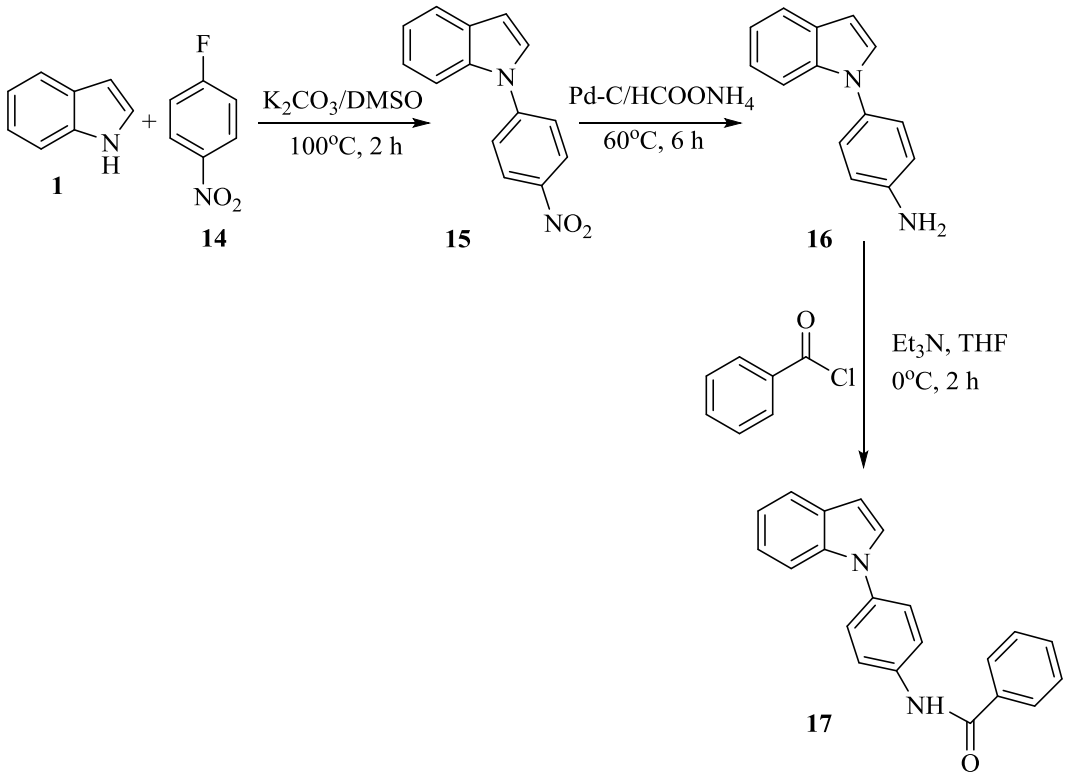

Scheme 4: Synthesis of indolyl amide using benzoyl chloride

4-Methoxy indolyl amide derivative **18** was synthesized starting from 4-methoxy benzoic acid utilizing HBTU coupling in basic conditions with catalytic DMAP (**Scheme 5**).

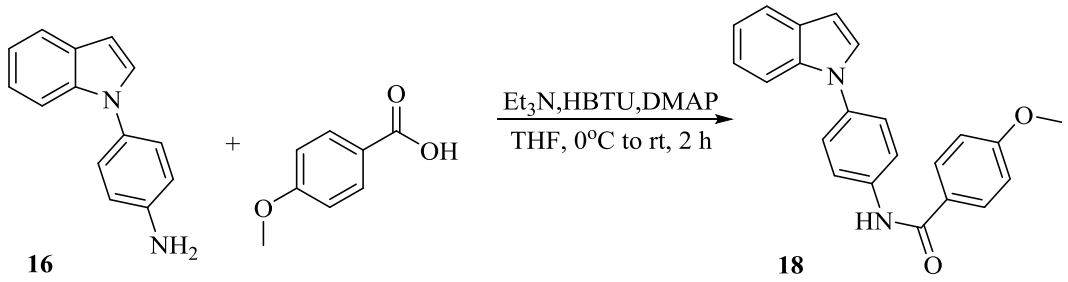

16 18

Scheme 5: Synthesis of indolyl amides using benzoic acids

Indolyl amido aldehydes **19** and **20** were synthesized using corresponding amides via Vilsmeier haack formylation with $POCl_3$ (**Scheme 6**).

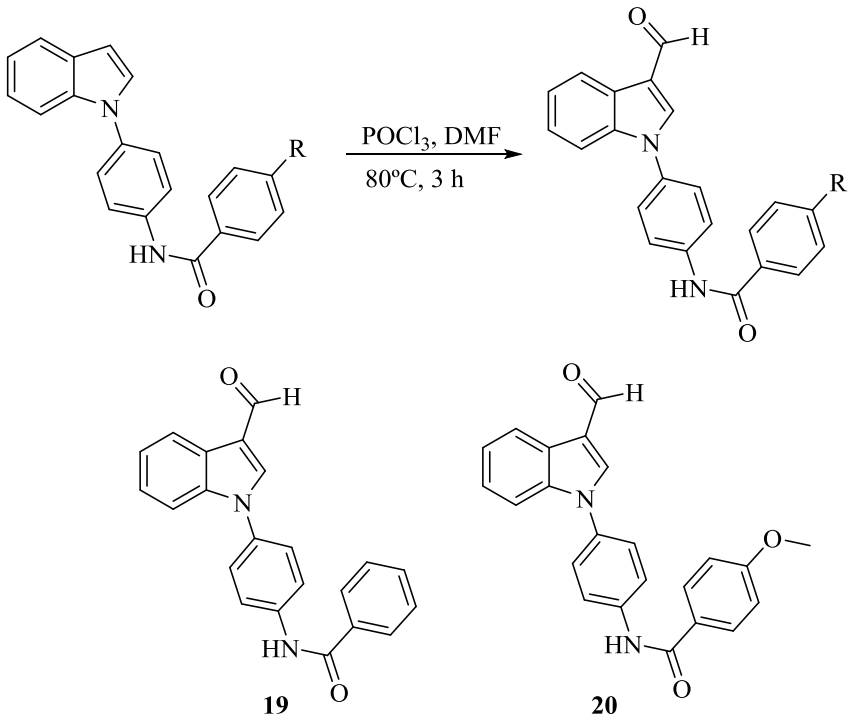

Scheme 6: Synthesis of indolyl amido aldehydes

Indolyl amido cyanoacrylic acids **21** and **22** were obtained via Knoevenagel condensation with corresponding indole amido aldehydes **19** and **20** using cyanoacetic acid in presence of piperidine (**Scheme 7**).

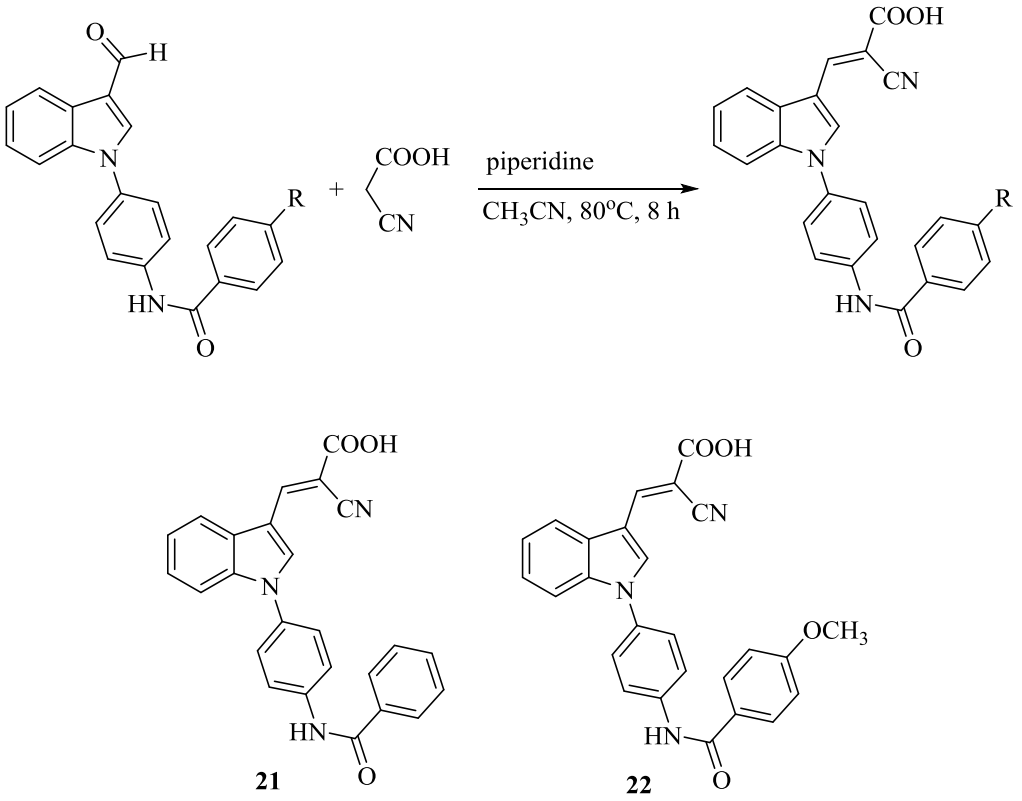

Scheme 7: Synthesis of indole amido cyanoacrylic acids

Cytotoxicity evaluation of indolyl amide derivatives:

To evaluate the biological activity of indolyl amide derivatives, we carried out cytotoxicity studies based on 3-[4,5-dimethylthiazol-2-yl]-2,5- diphenyltetrazolium bromide (MTT) assay. This assay measures cell viability based on the conversion of MTT to insoluble purple formazan via cleavage of the tetrazolium ring of MTT by the action of mitochondrial reductase in living cells.

MDA-MB-231 and 4T1 cell lines were chosen for preliminary cytotoxicity studies. We have chosen these two cell lines because we are targeting MCT1 and MCT4 for the inhibition of glycolysis. MDA-MB-231 is a triple negative breast cancer cell line that predominantly expresses MCT4, and 4T1 is a murine stage IV metastatic breast cancer cell line that predominantly expresses MCT1. The test results indicate that all the compounds **15-22** are non-cytotoxic in MDA-MB-231 and 4T1 cell lines even at 25 µM concentration (**Table 2**). MCT1 IC50 values of compounds **21** and **22** will be evaluated in the future.

Table 2: IC_{50}* values of indole derivatives in MDA-MB-231 and 4T1 cell lines using MTT assay

Compound No.	**Compound**	**MDA-MB-231**	**4T1**
17	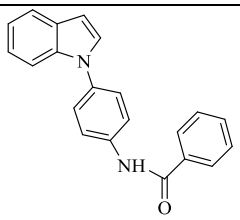	>25	>25
18	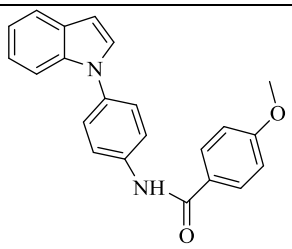	>25	>25

19	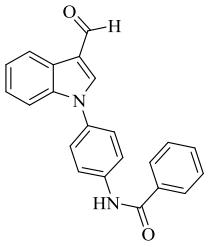	>25	>25
20	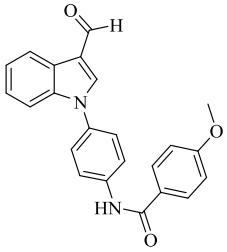	>25	>25
21	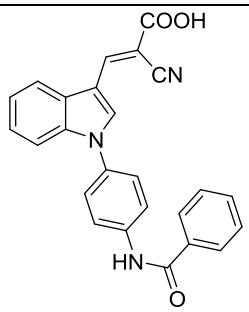	>25	>25
22	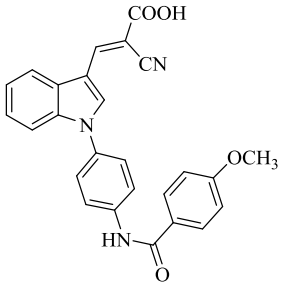	>25	>25

*IC_{50} is expressed in avg±SEM µM, average of 3 experimental values

CHAPTER 3: EXPERIMENTAL PROCEDURES AND SPECTRAL CHARACTERIZATION

Synthesis of indole cyanoacrylic acids

To a mixture of 1H-indole **1** (10 mmol) in DMF (60 mmol) was added $POCl_3$ (12 mmol) at 0 ^oC and the reaction mixture was heated at 80 ^oC for 3 hours. Upon completion (TLC), the reaction mixture was poured into a saturated solution of Na_2CO_3 at 90 ^oC and stirred for 1 hour. The solid obtained was filtered and washed with ether and hexane mixture to obtain the 1H-indole-3-carbaldehyde **2**. To a solution of aldehyde **2** (1 mmol) and cyanoacetic acid (1.5 mmol) in acetonitrile (10 mL), piperidine (1.3 mmol) was added and the reaction mixture was refluxed at 80 ^oC for 8 hours. After conformation that the reaction was complete, the mixture was poured in 20 mL of ice-cold 3N HCl and stirred for 20 minutes. The resulting solid was collected by filtration and washed with hexanes. The solid was suspended in chloroform (10 mL) and stirred overnight to remove the impurities. Finally pure product **3** was obtained upon filtration in 69% yield.

Compound 3: (E)-2-cyano-3-(1H-indol-3-yl)acrylic acid

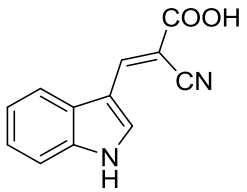

^{1}H NMR (500 MHz, DMSO-d_6): δ 12.55 (s, 1H), 8.58-8.53 (m, 2H), 7.98-7.93 (m, 1H), 7.60 (d, *J* = 8.5 Hz, 1H), 7.30 (m, 2H).

^{13}C NMR (125 MHz, DMSO-d_6): δ 165.13, 146.62, 136.67, 132.53, 127.39, 124.01, 122.51, 118.94, 113.34, 110.30, 94.16.

Representative procedure for synthesis of (E)-2-cyano-3-(1-(4-substituted benzyl)-1H-indol-3-yl)acrylic acids:

To synthesize substituted benzyl bromides, substituted benzaldehyde (10 mmol) was dissolved in THF (20 mL) and cooled to 0 ^{o}C and $NaBH_4$ (5 mmol) was added very slowly and the reaction was completed in 30 mins. To the substituted benzyl alcohol (10 mmol) in diethylether (20 mL) was added PBr_3 (3 mmol) dropwise very slowly at 0 ^{o}C. The reaction mixture was quenched with saturated $NaHCO_3$ and extracted with ether-water. The organic layers were collected, dried with anhydrous $MgSO_4$ and evaporated under vacuum to obtain substituted benzyl bromide.

To a mixture of 1H-indole **1** (10 mmol) in DMSO (10 mL) was added benzyl bromide (20 mmol) and K_2CO_3 (20 mmol) and stirred at 100 ^{o}C overnight. Upon the completion of the reaction, the reaction mixture was poured into water and stirred to obtain solid, which was then filtered and washed with hexanes to yield 1-(4-benzylphenyl)-1H-indole. To a mixture of this benzylated indole and DMF (60 mmol), $POCl_3$ (12 mmol) was added dropwise at 0 ^{o}C and the reaction mixture was heated at 80 ^{o}C for 3 hours. Upon completion (TLC), the reaction mixture was poured into a saturated solution of Na_2CO_3 at 90 ^{o}C and stirred for 1 hour. The solid obtained was filtered and washed with ether and hexane mixture to obtain the 1-(4-benzylphenyl)-1H-indole-3-carbaldehyde. To this aldehyde (1 mmol) and cyanoacetic acid (1.5 mmol) in acetonitrile (10 mL), piperidine (1.3 mmol) was added and the reaction mixture was refluxed at 80 ^{o}C for 8 hours. After conformation that the reaction was complete, the mixture was poured in 20 mL of ice-cold 3N HCl and stirred for 20 minutes. The resulting solid was collected by filtration and washed with hexanes. The solid was suspended in chloroform (10 mL)

and stirred overnight to remove the impurities. Finally pure product **4** was obtained upon filtration in 57% yield.

Compound 4: (E)-3-(1-benzyl-1H-indol-3-yl)-2-cyanoacrylic acid

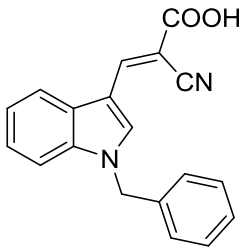

^{1}H NMR (500 MHz, DMSO-d_6): δ 8.61 (s, 1H), 8.46 (s, 1H), 7.87 (d, *J* = 7.0 Hz, 1H), 7.55 (d, *J* = 7.0 Hz, 1H), 7.29-7.25 (m, 7H), 5.54 (s, 2H).

^{13}C NMR (125 MHz, DMSO-d_6): δ 165.33, 146.08, 137.02, 136.79, 135.01, 129.50, 128.64, 128.31, 127.97, 124.51, 123.21, 119.41, 118.96, 112.35, 110.06, 94.95, 50.79.

Compound 5: (E)-2-cyano-3-(1-(4-ethylbenzyl)-1H-indol-3-yl)acrylic acid

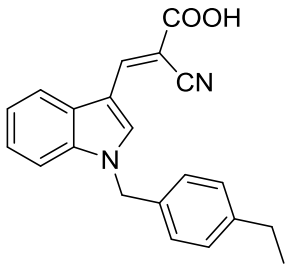

^{1}H NMR (500 MHz, DMSO-d_6): δ 8.68 (s, 1H), 8.52 (s, 1H), 7.97 (d, *J* = 7.5 Hz, 1H), 7.64 (d, *J* = 7.5 Hz, 1H), 7.33-7.17 (m, 6H), 5.60 (s, 2H), 2.57-2.51 (m, 2H), 1.12 (t, *J* = 6.0 Hz, 3H).

^{13}C NMR (125 MHz, DMSO-d_6): δ 165.33, 146.04, 144.25, 136.93, 135.10, 134.55, 128.86, 128.46, 128.12, 124.47, 123.11, 119.55, 118.98, 112.55, 110.11, 95.12, 50.64, 28.54, 16.25.

Compound 6: (E)-2-cyano-3-(1-(4-methoxybenzyl)-1H-indol-3-yl)acrylic acid

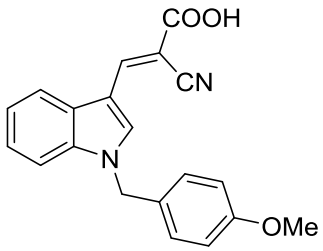

^{1}H NMR (500 MHz, DMSO-d_6): δ 8.67 (s, 1H), 8.51 (s, 1H), 7.97 (d, *J* = 7.5 Hz, 1H), 7.68 (d, *J* = 8.0 Hz, 1H), 7.34-7.27 (m, 4H), 6.92 (d, *J* = 8.5 Hz, 2H), 5.57 (s, 2H), 3.72 (s, 3H).

^{13}C NMR (125 MHz, DMSO-d_6): δ 165.28, 159.64, 146.07, 136.84, 134.95, 129.69, 129.06, 128.45, 124.38, 123.11, 119.50, 118.93, 114.88, 112.55, 110.01, 94.92, 55.80, 50.32.

Compound 7: (E)-3-(1-(4-chlorobenzyl)-1H-indol-3-yl)-2-cyanoacrylic acid

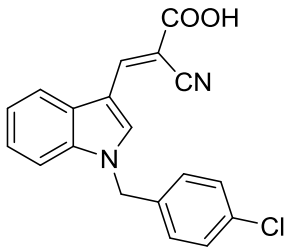

^{1}H NMR (500 MHz, DMSO-d_6): δ 8.70 (s, 1H), 8.52 (s, 1H), 7.97 (d, *J* = 8.0 Hz, 1H), 7.61 (d, *J* = 8.0 Hz, 1H), 7.42 (d, *J* = 8.0 Hz, 1H), 7.32-7.27 (m, 4H), 5.67 (s, 2H).

^{13}C NMR (125 MHz, DMSO-d_6): δ 165.23, 146.01, 136.80, 136.32, 135.07, 133.22, 129.91, 129.50, 128.41, 124.51, 123.19, 119.58, 118.85, 112.42, 110.20, 95.38, 50.03.

Compound 8: (E)-3-(1-(4-bromobenzyl)-1H-indol-3-yl)-2-cyanoacrylic acid

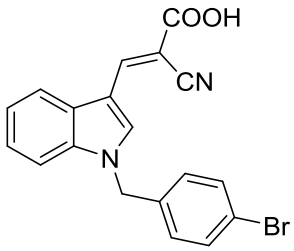

^{1}H NMR (500 MHz, DMSO-d_6): δ 8.70 (s, 1H), 8.52 (s, 1H), 7.98 (d, *J* = 7.0 Hz, 1H), 7.61 (d, *J* = 7.0 Hz, 1H), 7.57-7.54 (m, 2H), 7.33-7.24 (m, 4H), 5.66 (s, 2H).

^{13}C NMR (125 MHz, DMSO-d_6): δ 165.21, 146.03, 136.81, 136.76, 135.11, 132.42, 130.22, 128.41, 124.52, 123.20, 121.74, 119.59, 118.83, 112.42, 110.21, 95.35, 50.10.

Representative example for the synthesis of (E)-2-cyano-3-(1-(4-substituted phenyl)-1H-indol-3-yl)acrylic acids:

To a solution of 1H-indole **1** (10 mmol) in DMSO (25 mL), were added iodobenzene (15 mmol), K_2CO_3 (20 mmol), CuI (2 mmol), L-proline (1 mmol) and refluxed at 100 ^oC overnight. The reaction mixture was extracted in ethyl acetate-water mixture (3x100 mL) and the organic layers were collected and dried in anhydrous $MgSO_4$ and evaporated under vacuum. The resulting liquid was purified using column chromatography in ethyl acetate-hexanes mixture (1:9 ratio) to obtain 1-phenyl-1H-indole. To a solution of phenyl indole (10 mmol) and DMF (60 mmol), $POCl_3$ (12 mmol) was added dropwise at 0 ^oC and the reaction mixture was heated at 80 ^oC for 3 hours. Upon completion (TLC), the reaction mixture was poured into a saturated solution of Na_2CO_3 at 90 ^oC and stirred for 1 hour. The solid obtained was filtered and washed with ether and hexane mixture to obtain the 1-(4-benzylphenyl)-1H-indole-3-carbaldehyde. To this aldehyde (1 mmol) and cyanoacetic acid (1.5 mmol) in acetonitrile (10 mL), piperidine (1.3 mmol) was added and the reaction mixture was refluxed at 80 ^oC for 8 hours. After conformation that the reaction was complete, the mixture was poured in 20 mL of ice-cold 3N HCl and stirred for 20 minutes. The resulting solid was collected by filtration and washed with hexanes. The solid was suspended in chloroform (10 mL) and stirred overnight to remove the impurities. Finally pure product **9** was obtained upon filtration in 65% yield.

Compound 9: (E)-2-cyano-3-(1-phenyl-1H-indol-3-yl)acrylic acid

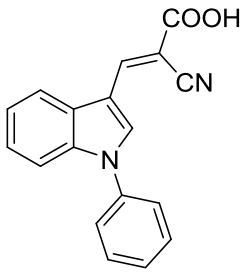

^{1}H NMR (500 MHz, DMSO-d_6): δ 8.63 (s, 1H), 8.60 (s, 1H), 8.10-8.09 (m, 1H), 7.71-7.66 (m, 4H), 7.59-7.56 (m, 2H), 7.39-7.38 (m, 2H).

^{13}C NMR (125 MHz, DMSO-d_6): δ 164.66, 138.72, 138.48, 135.89, 130.63, 129.83, 128.54, 128.31, 124.85, 124.38, 122.41, 121.42, 119.27, 112.01, 111.54, 108.90.

Compound 10: (E)-2-cyano-3-(1-(4-methoxyphenyl)-1H-indol-3-yl)acrylic acid

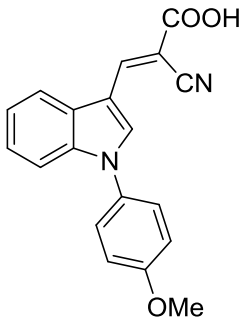

^{1}H NMR (500 MHz, DMSO-d_6): δ 8.60 (d, *J* = 8.0 Hz, 2H), 8.31 (s, 1H), 8.05-8.03 (m, 1H), 7.56 (d, *J* = 8.5 Hz, 2H), 7.47-7.45 (m, 1H), 7.36-7.34 (m, 2H), 7.18 (d, *J* = 8.5 Hz, 1H), 3.86 (s, 3H).

^{13}C NMR (125 MHz, DMSO-d_6): δ 165.05, 159.86, 145.85, 137.04, 134.12, 130.88, 128.27, 126.82, 125.10, 123.51, 119.80, 118.92, 115.88, 112.18, 111.28, 96.60, 56.26.

Compound 11: (E)-2-cyano-3-(1-(pyridin-2-yl)-1H-indol-3-yl)acrylic acid

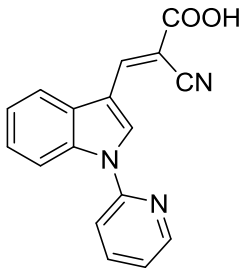

^{1}H NMR (500 MHz, DMSO-d_6): δ 8.95 (s, 1H), 8.62 (d, *J* = 4 Hz, 1H), 8.52 (s, 1H), 8.14 (d, *J* = 8 Hz, 1H), 8.00 (t, *J* = 7.5 Hz, 1H), 7.90 (s, 1H), 7.86 (d, *J* = 7 Hz, 1H), 7.68 (d, *J* = 8 Hz, 1H), 7.40-7.32 (m, 3H).

^{13}C NMR (125 MHz, DMSO-d_6): δ 164.80, 151.05, 149.71, 145.08, 139.87, 135.48, 131.18, 129.28, 125.25, 123.74, 122.96, 118.93, 118.23, 116.44, 114.17, 112.50, 98.50.

Compound 12: (E)-2-cyano-3-(1-(pyridin-3-yl)-1H-indol-3-yl)acrylic acid

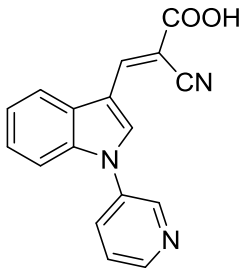

^{1}H NMR (500 MHz, DMSO-d_6): δ 9.13 (s, 1H), 8.87 (d, *J* = 5.0 Hz, 1H), 8.72 (s, 1H), 8.60 (s, 1H), 8.47 (d, *J* = 8.5 Hz, 1H), 8.13-8.11 (m, 1H), 7.93-7.91 (dd, *J* = 8.0, 5.0 Hz, 1H), 7.63-7.61 (m, 1H), 7.46-7.41 (m, 1H).

^{13}C NMR (125 MHz, DMSO-d_6): δ 164.74, 147.37, 145.78, 144.29, 136.73, 136.46, 135.81, 134.08, 128.35, 126.65, 125.61, 123.99, 120.17, 118.42, 112.41, 112.09, 98.24.

Compound 13: (E)-2-(3-(2-carboxy-2-cyanovinyl)-1H-indol-1-yl)benzoic acid

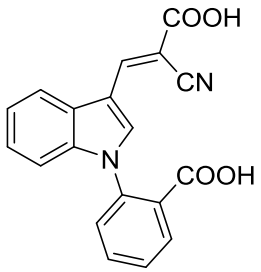

^{1}H NMR (500 MHz, DMSO-d_6): δ 8.62 (s, 1H), 8.54 (s, 1H), 8.10-8.08 (m, 2H), 7.86 (t, *J* = 7.5 Hz, 1H), 7.67-7.70 (m, 2H), 7.38-7.32 (m, 2H), 7.14 (d, *J* = 7.5 Hz, 1H).

^{13}C NMR (125 MHz, DMSO-d_6): δ 166.90, 165.04, 146.27, 138.28, 136.63, 135.50, 134.13, 132.04, 130.48, 130.12, 129.46, 127.74, 125.13, 123.35, 119.87, 118.89, 111.79, 111.34, 96.36.

Synthesis of 1-(4-nitrophenyl)-1*H*-indole:

A mixture of (1H)indole **1** (1.0 eq, 42.7 mmol) and 4-fluoro nitrobenzene **14** (1.1 eq, 46.9 mmol) were first stirred at room temperature in 30 mL DMSO, followed by the addition of K_2CO_3 (3 eq, 128 mmol). The reaction mixture was stirred for 12 hours at 90 ºC. After it was confirmed that the reaction was complete using a TLC (20% EtOAc/hexane), water was added to the reaction mixture in order to dissolve the excess potassium carbonate, and the resultant precipitate was collected by filtration. The yellow solid was washed with hexane to afford the product 1-(4-nitrophenyl)-1H-indole **15** in 80% yield.

Compound 15: 1-(4-nitrophenyl)-1H-indole

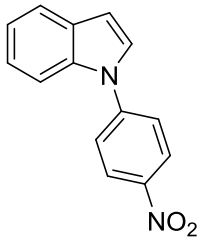

^{1}H NMR (500 MHz, DMSO-d_6): δ 8.40 – 8.38 (m, 2H), 7.73 (d, J= 7.5, 1H), 7.70-7.66 (m, 3H), 7.39 (d, J= 3Hz, 1H), 7.32 (t, J= 7.5Hz, 1H), 7.27 (t, J= 7.5Hz, 1H), 6.80 (t, J= 4Hz, 1H).

^{13}C NMR (125 MHz, DMSO-d_6): δ 145.23, 1335.26, 130.14, 127.14, 125.51, 123.37, 121.71, 121.62, 110.51, 106.20.

Synthesis of 4-(1*H*-indol-1-yl) aniline:

The above-formed 1-(4-nitrophenyl)-1*H*-indole **15** was reduced to obtain 4-(1*H*-indol-1-yl) aniline **16** by a catalytic hydrogenation using palladium charcoal catalyst and ammonium formate and THF (100 mL) as a solvent. Compound **15** (1 eq, 17.9 mmol) was dissolved in 50 mL THF. Then, Pd/C (0.3 eq, 75.2mmo) was added followed by addition of ammonium formate (6 eq, 107.5 mmol) and refluxed for 6 hours. The reaction mixture was cooled to room temperature. Finally, the reaction mixture was fast flushed through silica gel to get rid of excess ammonium formate and Pd/C and concentrated under vacuum to obtain **16** as a viscous, dark greenish compound in 83% yield.

Compound 16: 4-(1H-indol-1-yl)aniline

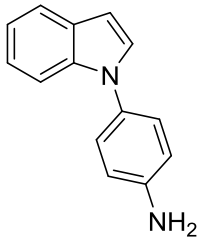

^{1}H NMR (500 MHz, DMSO-d_6): δ 8.18 (d, J= 6Hz, 1H), 7.93 (d, J= 7Hz, 1H), 7.66-7.7.63 (m, 3H), 7.54 (d, J= 8Hz, 2H), 7.10 (s, 1H), 3.77 (s, 2H).

^{13}C NMR (125 MHz, DMSO-d_6): δ 145.98, 136.98, 130.87, 129.46, 129.09, 126.31, 122.64, 121.62, 120.60, 116.00, 111.21, 103.10.

Synthesis of N-(4-(1H-indol-1-yl)phenyl)benzamide:

To a mixture of **16** (1.00 eq, 5.7 mmol) and triethylamine (3 eq, 17.1 mmol) dissolved in THF, benzoyl chloride (1.2 eq, 6.84 mmol) was added drop wise at 0 ˚C. The reaction mixture was brought back to room temperature and further stirred for 2 hours by which time the reaction was complete. The reaction mixture was extracted with ethyl acetate (EtOAc) and water followed by extraction with $NaHCO_3$ to quench any acid formation to get white precipitate. Finally, the solid was filtered and evaporated under vacuum, and was stirred overnight in ether and the resultant solid was filtered to obtain pure product **17** in 70% yield.

Compound 17: N-(4-(1H-indol-1-yl)phenyl)benzamide

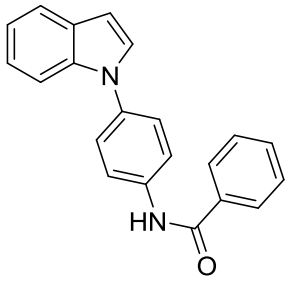

^{1}H NMR (500 MHz, DMSO-d_6): δ 8.12 (s, 1 H), 7.91 (d, J = 8.5 Hz, 2 H), 7.81 - 7.79 (m, 2 H), 7.71 (d, J = 7.5 Hz, 1 H), 7.59 - 7.54 (m, 2H), 7.52 - 7.48 (m, 2H), 7.32 (d, J = 3 Hz, 1H), 7.26 - 7.17 (m, 2H), 6.69 (d, J= 3.5, 1H).

^{13}C NMR (125 MHz, DMSO-d_6): δ 163.96, 149.76, 140.20, 136.82, 135.64, 129.33, 128.38, 127.83, 127.80, 124.91, 123.99, 122.53, 121.79, 121.27, 120.53, 110.33, 103.88.

Representative procedure for indole amides synthesized from corresponding acids.

Compound **16** (1eq, 4.85 mmol) was first dissolved in THF and cooled to 0 ˚C, followed by addition of triethylamine (3 eq, 14.55 mmol). Then, 4-methoxy benzoic acid (1.5 eq, 7.3 mmol) was added slowly to the reaction mixture at 0 ˚C. The reaction mixture was brought to room temperature before the addition of HBTU (1.6 eq, 7.76 mmol) and a catalytic amount of DMAP, and the reaction was complete after stirring for 2 hrs. The reaction mixture was extracted with EtOAc and water, and then some $NaHCO_3$ was added to the EtOAc/product extract to remove any acid formed and was dried by anhydrous $MgSO_4$. Finally the product was concentrated by rotary vacuum evaporation and was stirred overnight in $CHCl_3$ to remove impurities. Filtration of the product from $CHCl_3$ afforded the pure product **18** in 65% yield.

Compound 18: N-(4-(1H-indol-1-yl)phenyl)-4-methoxybenzamide

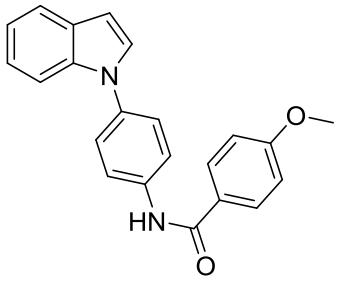

^{1}H NMR (500 MHz, DMSO-d_6): δ 10.30 (s, 1H), 8.02-7.98 (m, 4H), 7.65 (d, J= 8Hz, 1H), 7.62 (s, 1H), 7.57-7.54 (m, 3H), 7.21-7.18 (m, 1H), 7.13-7.07 (m, 3H), 6.68 (d, 3.5Hz, 1H), 3.85 (s, 3H).

^{13}C NMR (125 MHz, DMSO-d_6): δ 165.46, 162.45, 138.23, 135.69, 134.81, 130.13, 129.37, 129.00, 127.31, 124.57, 122.66, 121.79, 121.35, 120.56, 114.11, 110.80, 103.63, 55.91.

Representative procedure for synthesis of indolyl amido-aldehydes:

$POCl_3$ (2.5 eq, 0.65 mL) was slowly added at 0 ˚C to compound **17** (1 eq, 2.8 mmol) dissolved in N,N-dimethyl formamide (4 mL). The reaction mixture was refluxed at 80 ˚C for 3 hours, at which time TLC analysis (10% EtOAc/Hexane) indicated the completion of the reaction. The reaction mixture was poured in a saturated sodium carbonate solution and stirred for 30 minutes. The product was collected by filtration and was stirred in chloroform to remove the impurities and filtered again to obtain solid product **19** in 70% yield.

Compound 19: N-(4-(3-formyl-1H-indol-1-yl)phenyl)benzamide

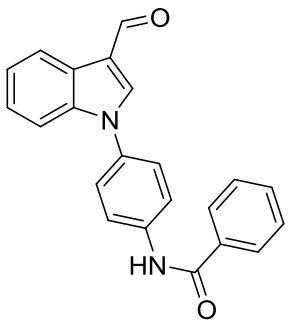

^{1}H NMR (500 MHz, DMSO-d_6): δ 10.57 (s, 1H), δ 10.03 (s, 1H), δ 8.57 (s, 1H), 8.21 (dd, J = 6.5 Hz, 1 H), 8.06 (d, J = 9 Hz, 2 H), 8.01 (d, J = 8.5Hz, 2 H), 7.67-7.65 (d, J = 10 Hz, 2 H), 7.61-7.60 (t, J = 5 Hz, 1 H), 7.67-7.54 (m, 6 H), 7.37-7.34 (m, 2 H).

^{13}C NMR (125 MHz, DMSO-d_6): δ 185.72, 166.28, 141.02, 139.51, 137.38, 135.16, 133.32, 132.23, 128.90, 128.20, 125.53, 125.48, 124.89, 123.65, 121.80, 119.08, 111.83.

Compound 20: N-(4-(3-formyl-1H-indol-1-yl)phenyl)-4-methoxybenzamide

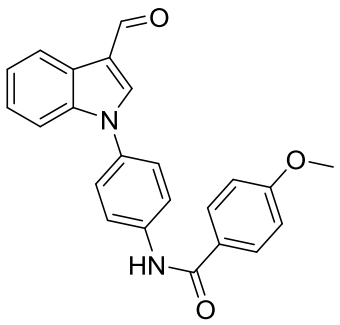

^{1}H NMR (500 MHz, DMSO-d_6): δ 10.11 (s, 1H), 8.38 (d, J= 8Hz, 1H), 8.08 (s, 1H), 7.92-7.87 (m, 6H), 7.52 (d, J= 8.5Hz, 2H), 7.47 (d, J= 7.5 Hz, 1H), 7.39-7.27 (m, 2H), 7.02-7.01 (d, J=9Hz, 2H), 3.89 (s, 3H).

^{13}C NMR (125 MHz, DMSO-d_6): δ 184.96, 165.38, 162.81, 138.24, 138.17, 137.63, 133.93, 129.04, 126.57, 125.58, 125.47, 124.64, 123.48, 122.23, 121.34, 119.61, 114.12, 111.03, 55.52.

Representative example for the synthesis of (E)-2-cyano-3-(1-(4-(4-sunstituted-benzamido)phenyl)-1H-indol-3-yl) acrylic acids:

To the aldehyde **19** (1 mmol) and cyanoacetic acid (1.5 mmol) in acetonitrile (10 mL), piperidine (1.3 mmol) was added and the reaction mixture was refluxed at 80 ^{o}C for 8 hours. After conformation that the reaction was complete, the mixture was poured in 20 mL of ice-cold 3N HCl and stirred for 20 minutes. The resulting solid was collected by filtration and washed with hexanes. The solid was suspended in chloroform (10 mL) and stirred overnight to remove the impurities. Finally pure product **21** was obtained upon filtration in 68% yield.

Compound 21: (E)-3-(1-(4-benzamidophenyl)-1H-indol-3-yl)-2-cyanoacrylic acid

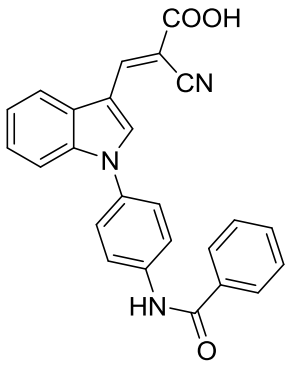

^{1}H NMR (500 MHz, DMSO-d_6): δ **^{1}H NMR (500 MHz, DMSO-d_6):** δ 10.54 (s, 1H), 8.57 (s, 1H), 8.55 (s, 1H), 8.05-7.97 (m, 5H), 7.66-7.54 (m, 6H), 7.37-7.34 (m, 2H).

^{13}C NMR (125 MHz, DMSO-d_6): δ 166.36, 164.75, 145.64, 139.75, 136.56, 135.07, 133.67, 133.08, 132.28, 128.9, 128.19, 128.06, 125.48, 125.04, 123.43, 121.92, 119.65, 118.64, 112.07, 111.24, 96.62.

Compound 22: (E)-2-cyano-3-(1-(4-(4-methoxybenzamido)phenyl)-1H-indol-3-yl) acrylic acid

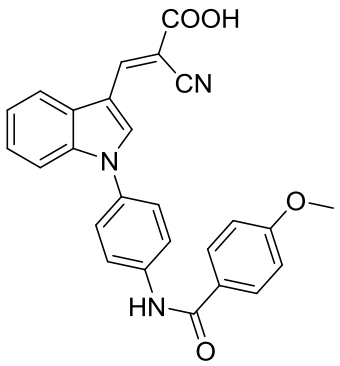

^{1}H NMR (500 MHz, DMSO-d_6): δ 10.38 (s, 1H), 8.57 (d, J= 10Hz, 2H), 8.06-7.99 (m, 5H), 7.65-7.63 (m, 1H), 7.56-7.54 (dd, J= 6Hz, 2H), 7.37-7.34 (m, 2H), 7.08-7.05 (m, 2H), 3.83 (s, 3H).

^{13}C NMR (125 MHz, DMSO-d_6): δ 165.62, 164.75, 162.53, 145.68, 140.03, 136.59, 133.71, 132.82, 130.19, 128.08, 127.11, 125.38, 124.99, 123.38, 121.74, 119.65, 118.62, 114.11, 112.09, 111.23, 96.49, 55.90.

CONCLUSION

MCTs play an important role in glycolysis that has many therapeutic implications in cancer treatment. In this regard, we have designed, synthesized and evaluated various indole derivatives as potential therapeutics for cancer. Indole cyanoacrylic acids and indolyl amide cyanoacrylic acids have been synthesized and characterized using NMR spectroscopy. We have also evaluated MCT1 inhibition of these derivatives in a non-cancerous RBE4 cell line. Most of the synthesized compounds were found to have potent MCT1 inhibition in the range of 12-100 nM, whereas compounds **1**, **11**, **12** and **13** did not show any activity. From these studies, compounds **9** and **10** were chosen as lead candidate compounds due to their potent MCT1 inhibition. Future studies include systemic toxicity study in healthy CD-1 mice, with further evaluation of anticancer efficacy in a tumor xenograft models.

REFERENCES

1. Hanahan, D.; Weinberg, R. A. "Hallmarks of Cancer: The Next Generation." *Cell*. **2011**, *144*, 646-674.
2. Cantor, J. R.; Sabatini, D. M. "Cancer Cell Metabolism: One Hallmark, Many Faces". *Canc Discov.* **2012**, *2*, 881-98.
3. Hsu, P. P.; Sabatini, D. M. "Cancer Cell Metabolism: Warburg and Beyond". *Cell*. **2008**, *134*, 703-707.
4. Ganapathy, V.; Thangarajue, M.; Parasad, P. D. "Nutrient transporters in cancer: Relevance to Warburg hypothesis and beyond". *Pharm & Ther*. **2009**, *121*, 29-40.
5. Rob A. C.; Isaac S. H.; Tak, W. M. "Regulation of cancer cell metabolism". *Nature Reviews Cancer*. **2009**, *11*, 85-95.
6. Olivier, F. "Pyruvate into lactate and back: From the Warburg effect to symbiotic energy fuel exchange in cancer cells". *Radiother and Onco*. **2009**, *92*, 329-333.
7. Warburg O. "On the origin of cancer cells". *Science*. **1956**, *123*, 309-14.
8. Vander, H. M. G.; Cantley, L C.; Thompson C. B. "Understanding the Warburg effect: the metabolic requirements of cell proliferation". *Science*. **2009**, *324*, 1029-1033.
9. Kim, H. H.; Kim, T.; Kim, E.; Park, J. K.; Park, S. J.; Joo, H.; Kim, J.H. "The Mitochondrial Warburg Effect: A Cancer Enigma" *Interdisciplinary Bio Central*. **2009**, *1*, 1-7.
10. Ganapathy-Kanniappan, S.; Geschwind, J. "Tumor glycolysis as a target for cancer therapy: progress and prospects". *Mol. Cancer*. **2013**, *12*, 152.

11. Pelicano, H.; Martin, D.; Xu, R.; Huang, P. "Glycolysis inhibition for anticancer treatment". *Oncogene*. **2006**, *25*, 4633-4646.
12. Kelloff, G. J.; Hoffman, J. M.; Johnson, B.; Scher, H. I.; Siegel, B. A.; Cheng, E. Y.; Cheson, B. D.; O'shaughnessy, J.; Guyton, K. Z.; Mankoff, D. A.; Shankar, L.; Larson, S. "M.; Sigman, C. C.; Schilsky, R. L.; Sullivan, D. C. "Progress and promise of FDG-PET imaging for cancer patient management and oncologic drug development." *Clin. Cancer Res.* **2005**, *11*, 2785–2808.
13. Som, P.; Atkins, H. L.; Bandoypadhyay, D.; Fowler, J. S.; MacGregor, R. R.; Matsui, K.; Oster, Z. H.; Sacker, D.F.; Shiue, C. Y.; Turner, H.; Wan, C. N.; Wolf, A. P.; Zabinski, S. V. "A fluorinated glucose analog, 2-fluoro-2-deoxy-D-glucose (F-18): Nontoxic tracer for rapid tumor detection" *Nucl. Med.* **1980**, *21*, 670–675.
14. Lu, H.; Forbes, R. A.; Verma, A. "Hypoxia-inducible Factor 1 Activation by Aerobic Glycolysis Implicates the Warburg Effect in Carcinogenesis". *Biol. Chem*. **2002**, *277*, 23111-5.
15. Ward, C.; Langdon, S. P.; Mullen, P.; Harris, A. L.; Harrison, D. J.; Supuran, C T.; Kunkler, I. H. "New strategies for targeting the hypoxic tumour microenvironment in breast cancer". *Cancer Treatment Reviews* **2013**, *39*, 171–179.
16. Sonveaux, P.; Vegran, F.; Schroeder, T.; Wegrin, M. C.; Verrax, J.; Rabbini, Z. N.; De Saedler, C. J.; Kennedy, K.M.; Diepart, C.; Jordan, B.F.; Kelley, M.J.; Gallez, B.; Wahl, M.L.; Feron, O.; Dewhirst, M. W. "Targeting lactate-fueled

respiration selectively kills hypoxic tumor cells in mice" *Clin. Inv*. **2008**, *11*, 3930-3942.

17. Halestrap, A. P.; Price, N. T. "The proton-linked monocarboxylate transporter (MCT) family: structure, function and regulation". *Biochem*. **1999**, *343*, 281–299.
18. Spanier, J. A.; Drewes, L. R. "Monocarboxylate Transporters in Drug Transporters: Molecular Characterization and Role in Drug Disposition (eds G. You and M. E. Morris), John Wiley & Sons, Inc., Hoboken, NJ, USA. **2007**, 147-170.
19. Pinheiro, C.; Longatto-Filho, A.; Azevedo-Silva, J.; Casal, M.; Schmitt, F. C.; Baltazar, F. "Role of monocarboxylate transporters in human cancers: state of the art". *Bioenerg. Biomembr*. **2012**, *44*, 127-39.
20. Enerson, B. E.; Drewes L.R. "Molecular features, regulation, and function of monocarboxylate transporters: implications for drug delivery". *Pharm. Sci*. **2003,** *92*, 1531-44.
21. Morris, M. E.; FelmLee, M. A. "Overview of the proton-coupled MCT (SLC16A) family of transporters: characterization, function and role in the transport of the drug of abuse gamma-hydroxybutyric acid". *AAPS J*. **2008**, *10*, 311-21.
22. Arend, B. "The expression of lactate transporters MCT1 and MCT4 in heart and muscle". *Applied Physiology*. **2001**, *86*, 6-11.
23. Ullah, M. S.; Davies A. J.; Halestrap, A. P. "The plasma membrane lactate transporter MCT4, but not MCT1, is up-regulated by hypoxia through a HIF-1alpha-dependent mechanism". *Biol. Chem*. **2006**, *281*, 9030–9037.

24. Sonveaux, P.; Copetti, T.; Saedeleer, C. J. D.; Vegran, F.; Verrax, J.; Kennedy, K. M.; Moon, E. J.; Dhup, S.; Danhier, P.; Frerart, F.; Gallez, B.; Ribeiro, A.; Michiels, C.; Dewhirst, M. W.; Feron, O. "Targeting the Lactate Transporter MCT1 in Endothelial Cells Inhibits Lactate-Induced HIF-1 Activation and Tumor Angiogenesis" *PLoS ONE*. **2012**, *7*, e33418.

25. Doherty, J. R.; Yang. C.; Scott, K. E.; Cameron, M. D.; Fallahi, M.; Li, W.; Hall, M. A.; Amelio, A. L.; Mishra, J. K.; Li, F.; Tortosa, M.; Genau, H. M.; Rounbehler, R. J.; Lu, Y.; Dang, C. V.; Kumar, K. G.; Butler, A. A.; Bannister, T. D.; Hooper, A. T.; Unsal-Kacmaz, K.; Roush, W. R.; Cleveland, J. L. "Blocking Lactate Export by Inhibiting the Myc Target MCT1 Disables Glycolysis and Glutathione Synthesis" *Cancer Res*. **2014**, *4*, 908-20.

26. Critchlow, S. E.; Tate, L. "Use of a MCT1 Inhibitor in the Treatment of Cancers Expressing MCT1 over MCT4". *PCT Int. Appl*. **2010**, WO 2010089580 A1 20100812.

27. Draoui, N.; Schicke, O.; Fernandes, A.; Drozak, X.; Nahra, F.; Dumont, A.; Douxfils, J.; Hermans, E.; Dogné, J. M.; Corbau, R.; Marchand, A.; Chaltin, P.; Sonveaux, P.; Feron, O.; Riant, O. "Synthesis and pharmacological evaluation of carboxycoumarins as a new antitumor treatment targeting lactate transport in cancer cells" *Bioorg. Med. Chem*. **2013**, *21*, 7107–7117.

28. Pertega-Gomes, N.; Vizcaino, J. R.; Miranda-Goncalves, V.; Pinheiro, C.; Silva, J.; Pereira, H.; Monteiro, P.; Henrique, R. M.; Reis, R. M.; Lopes, C.; Baltazar, F. "Monocarboxylate transporter 4 (MCT4) and CD147 overexpression is associated with poor prognosis in prostate cancer". *BMC Cancer*. **2011**, *11*, 1-9.

29. Hao, J.; Chen, H.; Madigan, M. C.; Cozzi, P. J.; Beretov, J.; Xiao, W.; Delprado, W. J.; Russell, P. J.; Li, Y. "Co-expression of CD147 (EMMPRIN), CD44v3-10, MDR1 and monocarboxylate transporters is associated with prostate cancer drug resistance and progression". *Br. J. Cancer.* **2010,** *103*, 1008-1018.
30. Sanita, P.; Capulli, M.; Teti, A.; Galatioto, G. P.; Vicentini, C.; Chiarugi, P.; Bologna, M.; Angelucci, A. "Tumor-stroma metabolic relationship based on lactate shuttle can sustain prostate cancer progression". *BMC Cancer*. **2014**, *14*, 1-14.
31. Wang, H.; Yang, C.; Doherty, J. R.; Roush, W. R.; Cleveland, J. L.; Bannister, T. D. "Synthesis and Structure Activity Relationships of Pteridine Dione and Trione Monocarboxylate Transporter 1 Inhibitors". *Med. Chem*. **2014**, *57*, 7317-7324.
32. Baek, G.; Tse, Y. F.; Hu, Z.; Cox, D.; Buboltz, N.; McCue, P.; Yeo, C. J.; White M. A.; DeBerardinis, R. J.; Knudsen, E. S.; Witkiewicz, A. K. "MCT4 defines a glycolytic subtype of pancreatic cancer with poor prognosis and unique metabolic dependencies". *Cell Rep*. **2014**, *9*, 2233-49.
33. Agnieszka, K. W.; Whitaker-Menezes, D.; Dasqupta, A.; Philp, N. J.; Lin, Z.; Gandara, R.; Sneddon, S.; Martinez-Outschoorn, U. E.; Sotqia, F.; Lisanti, M. P. "Reverse warburg Effect to identify high-risk breast cancer patients: stromal MCT4 predicts poor clinical outcome in triple-negative breast cancers". *Cell Cycle*. **2012**, *11*, 1108-1117.
34. Pavlides, S.; Whitaker-Menezes, D.; Castello-Cros, R.; Flomenberg, N.; Witkiewicz, A. K.; Frank, P.G.; Casimiro, M.C.; Wang, C.; Fortina, P.; Addya, S.; Pestell, R. G.; Martinez-Outschoorn, U.E.; Sotgia, F.; Lisanti, M.P. "The

reverse Warburg effect: Aerobic glycolysis in cancer associated fibroblasts and the tumor stroma". *Cell Cycle*. **2009**, *8*, 3984-4001.

35. Martinez-Outschoorn, U. E.; Pavlides, S.; Howell, A.; Pestell, R.G.; Tanowitz, H.B.; Sotgia, F.; Lisanti, M.P. "Stromal–epithelial metabolic coupling in cancer: Integrating autophagy and metabolism in the tumor microenvironment". *Int. J. Biochem. Cell Biol.* **2011**, *43*, 1045–1051.
36. Witkiewicz, A. K.; Casimiro, M. C.; Dasgupta, A.; Mercier, I.; Wang, C.; Bonuccelli, G. "*Towards a new "stromal based" classification system for human breast cancer prognosis and therapy*". *Cell Cycle*. **2009**, *8*, 1654-8.
37. Ontilo, A.A.; Engel, J.M.; Greenlee, R.T.; Mukesh, B.N. "Breast cancer subtypes based on ER/PR and Her2 expression: Comparison of clinicopathologic features and survival". *Clin Med & Res*. **2009**, *7*, 4-13.
38. De Laurentiis, M.; Cianniello, D.; Caputo, R.; Stanzione, B.; Arpino, G.; Cineri, S.; Lorusso, V.; De Placido, S. "Treatment of triple negative breast cancer (TNBC): current options and future perspectives". *Canc Tre Rev*. **2010**, *36S3*, S80–S86.
39. Tennant, D.A.; Durant, R.V.; Gottlieb, E. "Targeting metabolic transformation for cancer therapy". *Nature Reviews Cancer*. **2010**, *10*, 267-277.
40. Doherty, J.R.; Cleveland, J.L. "Targeting lactate metabolism for cancer therapeutics". *J. Clin. Investigation*. **2013**, *123*, 3685-92.
41. Halestrap, A. P.; Denton, R.M. "Specific Inhibition of Pyruvate Transport in Rat Liver Mitochondria and Human Erythrocytes by a-Cyano-4-hydroxycinnamate" *Biochem. J.* **1974**, *138*, 313-316.

42. Colen, C. B.; Shen, Y.; Ghoddoussi, F.; Yu, P.; Francis, T. B.; Koch, B. J.; Monterey, M.D.; Galloway, M.P.; Sloan, A.E.; Mathupala, S.P. "Metabolic targeting of lactate efflux by malignant glioma inhibits invasiveness and induces necrosis: an in vivo study". *Neoplasia*. **2011**, *13*, 620-32.
43. Bola, B.M.; Chadwick A. L.; Michopoulos, F.; Blount, K.G.; Telfer, B.A.; Williams, K.J.; Smith, P.D.; Critchlow, S.E.; Stratford, I. J. "Inhibition of monocarboxylate transporter-1 (MCT1) by AZD3965 enhances radiosensitivity by reducing lactate transport". *Mol. Cancer. Ther.* **2014**, *13*, 2805-16.
44. Gurrapu, S.; Jonnalagadda, S. K.; Alam, M. A.; Nelson, G. L.; Sneve, M. G.; Drewes, L. R.; Mereddy, V. R. "Monocarboxylate Transporter 1 Inhibitors as Potential Anticancer Agents". *ACS Med. Chem. Lett*. **2015**, *6*, 558−561.
45. Young, V. R. "Adult amino acid requirements: the case for a major revision in current recommendations". *J Nutr.* **1994**, *124(8 Suppl)*, 1517S-1523S.
46. Jones, R. S. "Tryptamine: a neuromodulator or neurotransmitter in mammalian brain?" *Progress in neurobiology*. **1982**, *19*, 117–139.
47. Young, S.N. "How to increase serotonin in the human brain without drugs". *Rev. Psychiatr. Neurosci*. **2007**, *32*, 394–99.
48. Kaushik, N. K.; Kaushik, N.; Attri, P.; Kumar, N.; Kim, C.H.; Verma, A. K.; Choi, E. H. "Biomedical importance of indoles". *Molecules*. **2013**, *18*, 6620-62.

Appendix

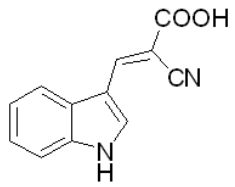
COOH
CN
N
H

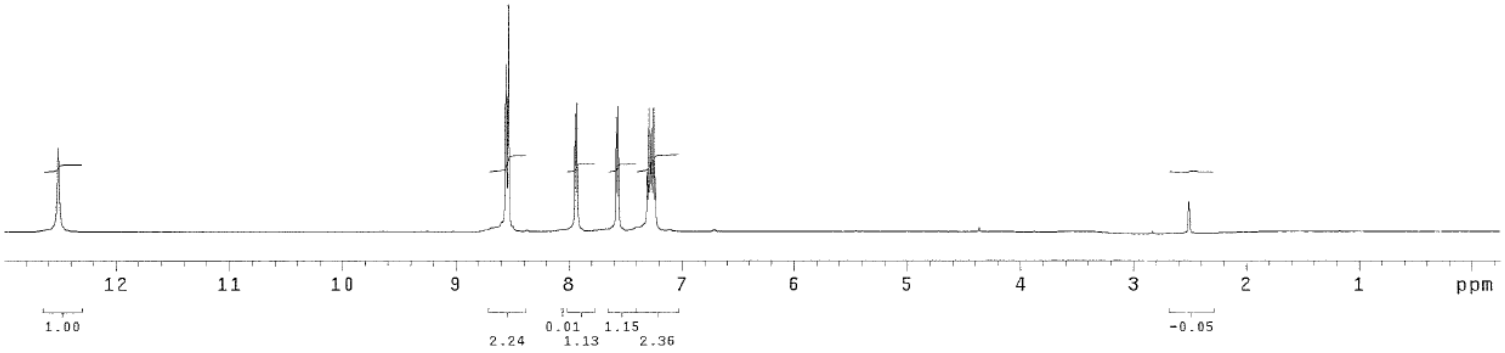
12
11
10
9
8
7
6
5
4
3
2
1
ppm
1.00
2.24
0.01
1.13
1.15
2.36
-0.05

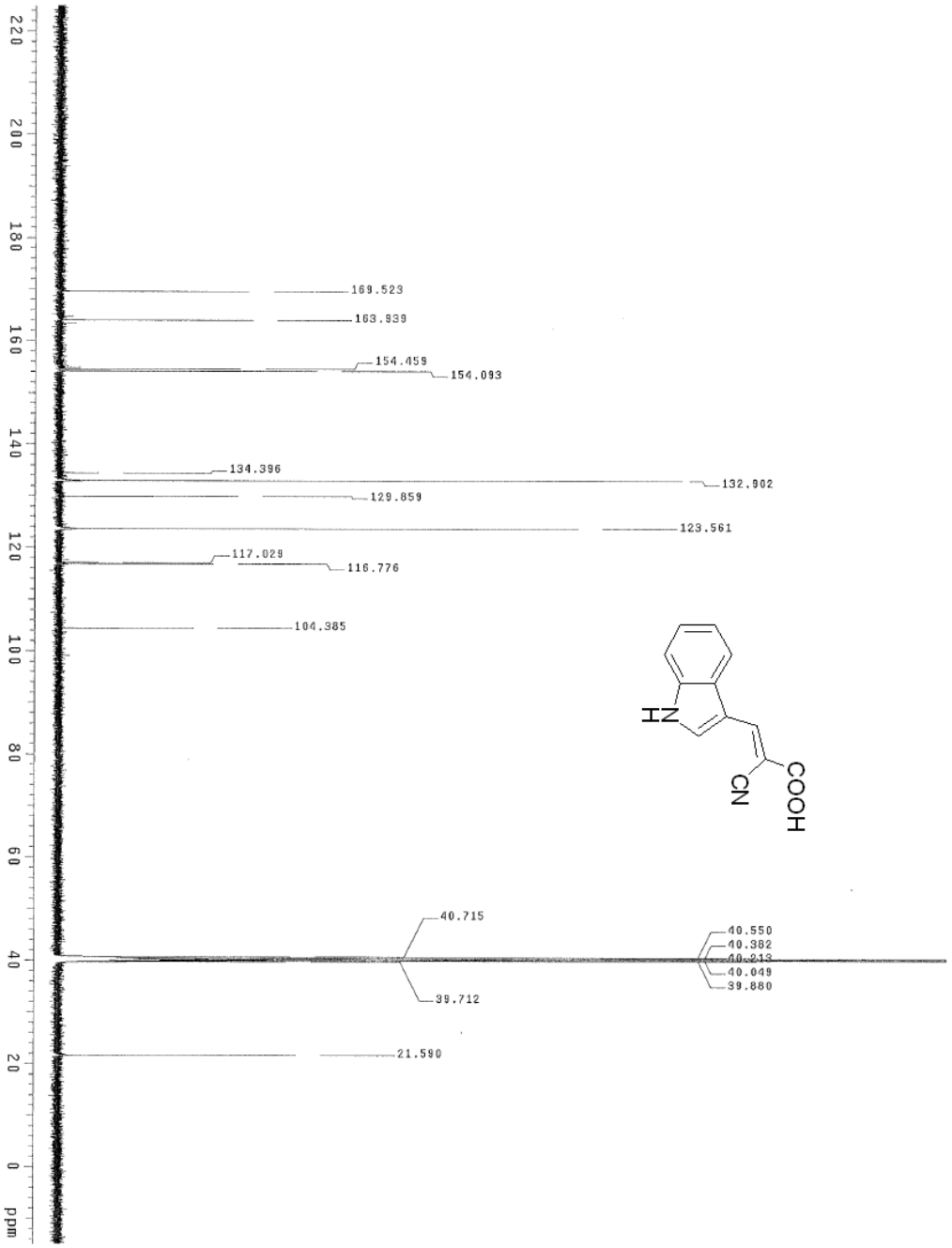
220
200
180
160
140
120
100
80
60
40
20
0
ppm
169.523
163.939
154.459
154.093
134.396
132.902
129.859
123.561
117.029
116.776
104.385
40.715
40.550
40.382
40.213
40.049
39.880
39.712
21.590
HN
CN
COOH

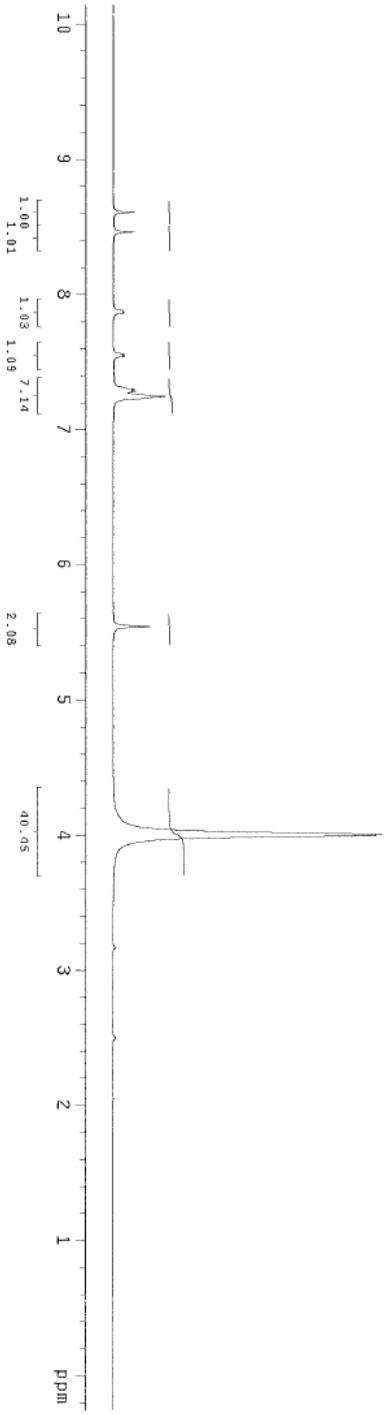
10
9
8
7
6
5
4
3
2
1
ppm
1.00
1.01
1.03
1.09
7.14
2.08
40.05

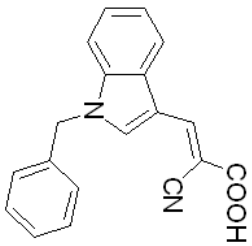
N
CN
COOH

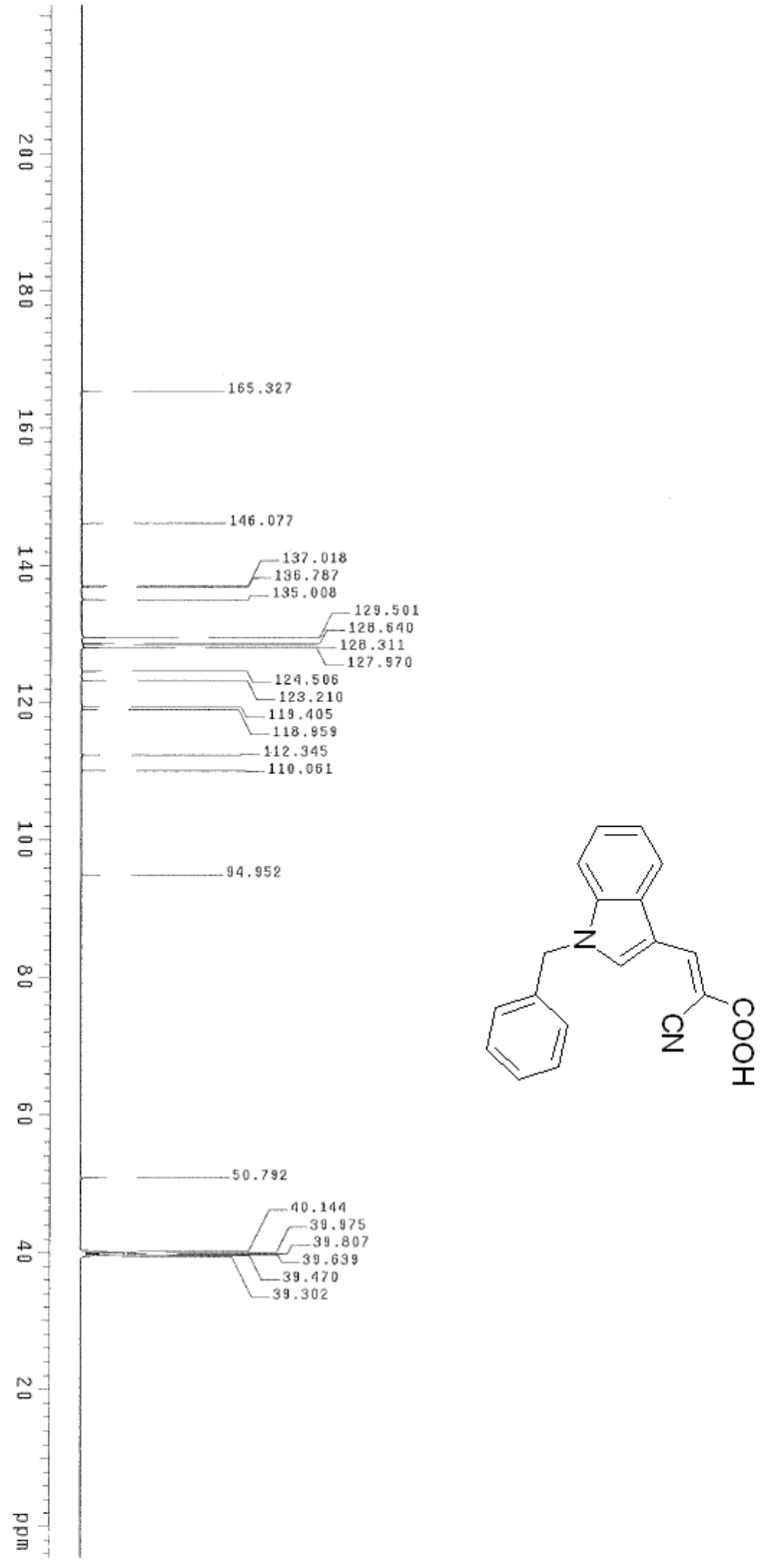
165.327
146.077
137.018
136.787
135.008
129.501
128.640
128.311
127.970
124.506
123.210
119.405
118.959
112.345
110.061
94.952
50.792
40.144
39.975
39.807
39.639
39.470
39.302
200
180
160
140
120
100
80
60
40
20
ppm
N
CN
COOH

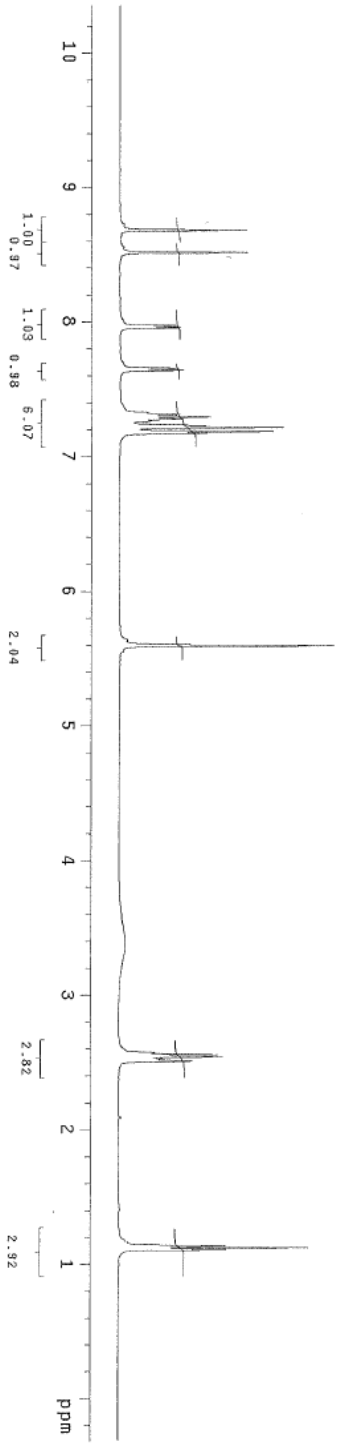
10
9
8
7
6
5
4
3
2
1
ppm
1.00
0.97
1.03
0.98
6.07
2.04
2.82
2.92

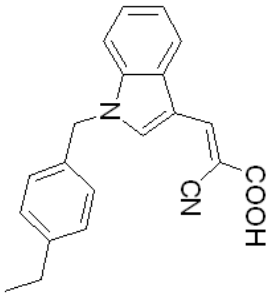
N
CN
COOH

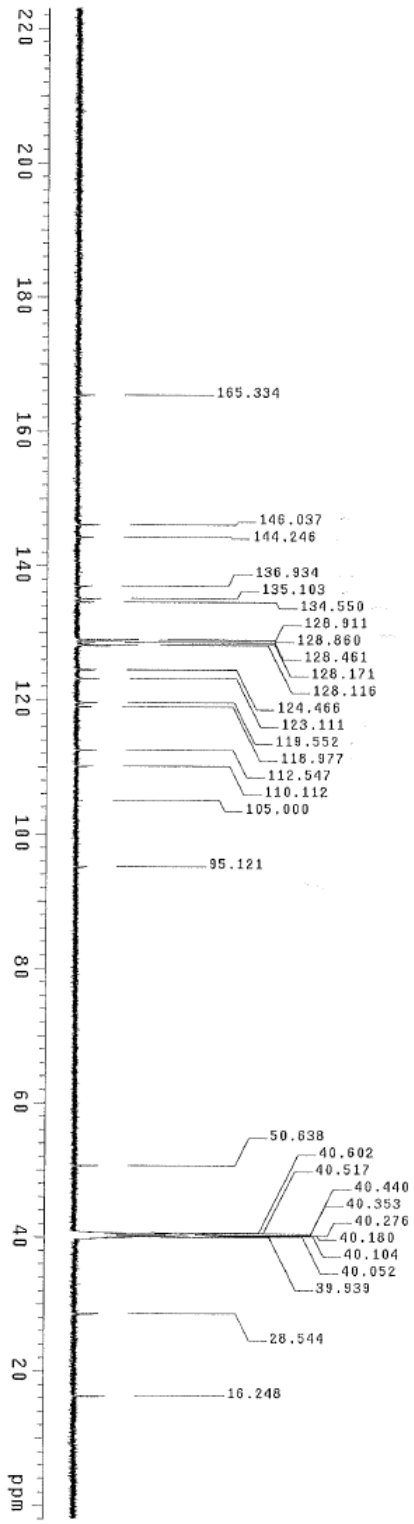
220
200
180
160
140
120
100
80
60
40
20
ppm
165.334
146.037
144.246
136.934
135.103
134.550
128.911
128.860
128.461
128.171
128.116
124.466
123.111
119.552
118.977
112.547
110.112
105.000
95.121
50.638
40.602
40.517
40.440
40.353
40.276
40.180
40.104
40.052
39.939
28.544
16.248

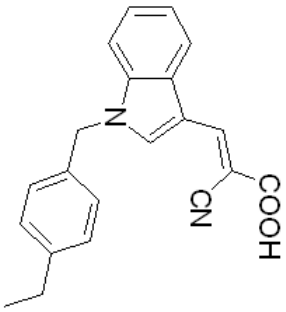
N
CN
COOH

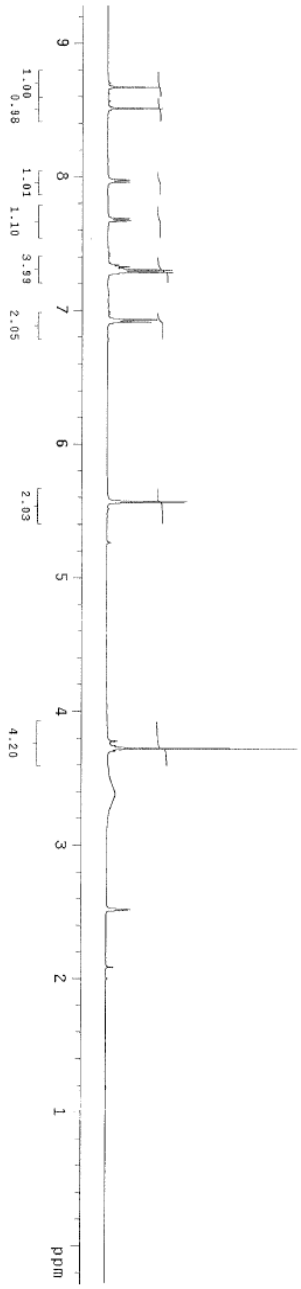
9
8
7
6
5
4
3
2
1
ppm
1.00
0.98
1.01
1.10
3.99
2.05
2.03
4.20

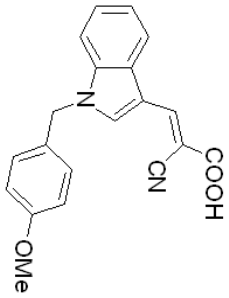
N
COOH
CN
OMe

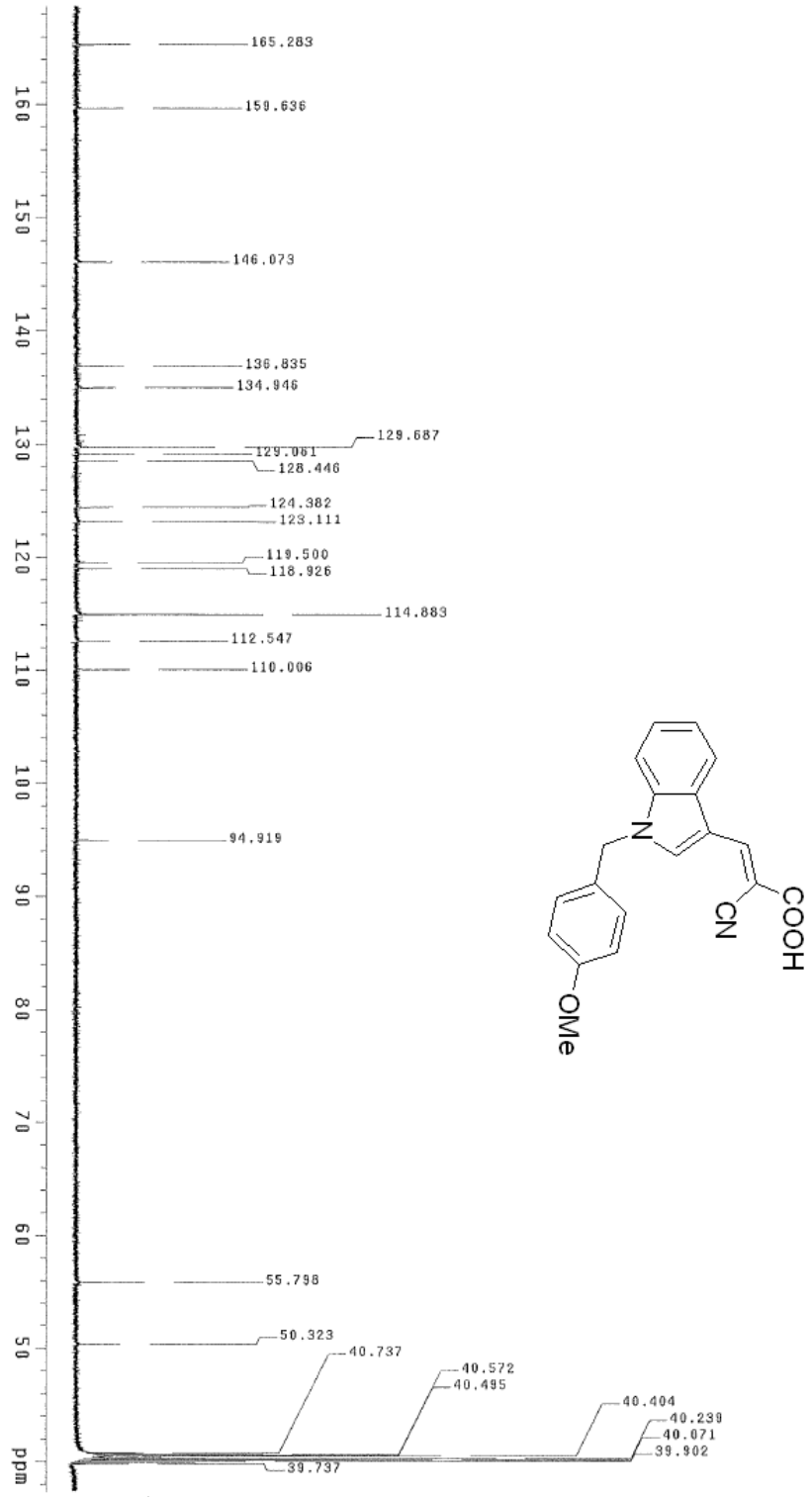
165.283
159.636
146.073
136.835
134.946
129.687
129.061
128.446
124.382
123.111
119.500
118.926
114.883
112.547
110.006
94.919
55.798
50.323
40.737
40.572
40.485
40.404
40.239
40.071
39.902
39.737
ppm
160
150
140
130
120
110
100
90
80
70
60
50
N
CN
COOH
OMe

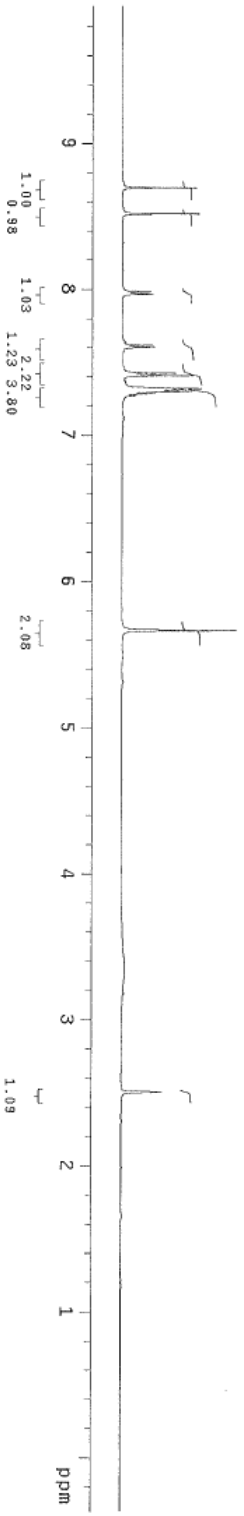
9
8
7
6
5
4
3
2
1
ppm
1.00
0.98
1.03
2.22
1.23
3.80
2.08
1.09

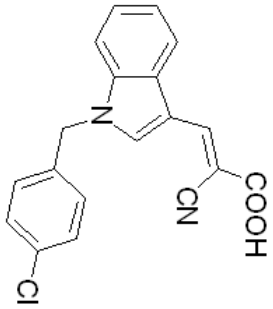
N
CN
COOH
Cl

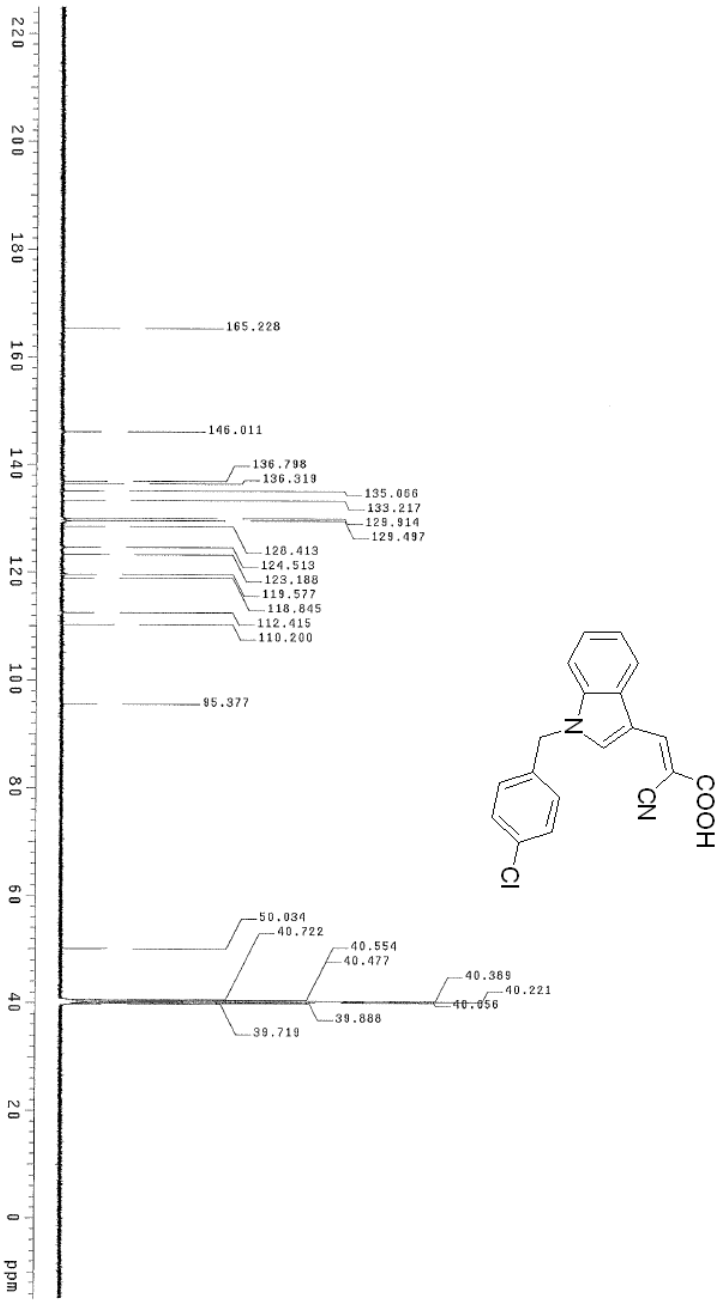
220
200
180
160
140
120
100
80
60
40
20
0
ppm
165.228
146.011
136.798
136.319
135.066
133.217
129.914
129.497
126.413
124.513
123.188
119.577
118.845
112.415
110.200
95.377
50.034
40.722
40.554
40.477
40.389
40.221
40.056
39.888
39.719
N
CN
COOH
Cl

10
9
8
7
6
5
4
3
2
1
ppm
1.00
0.98
1.01
2.96
4.10
2.06
2.90
1.83

N
COOH
CN
Br

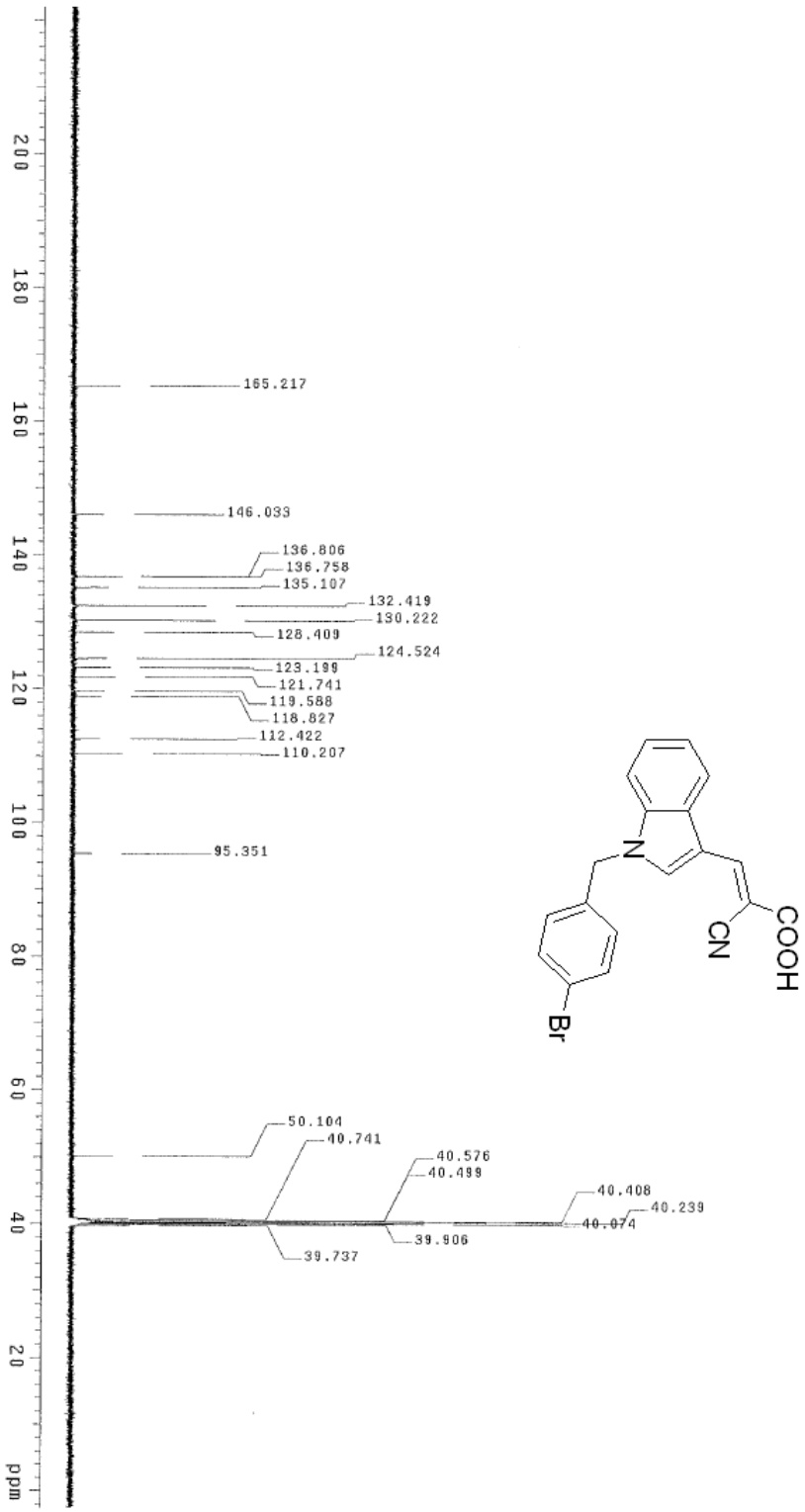
165.217
146.033
136.806
136.758
135.107
132.419
130.222
128.409
124.524
123.199
121.741
119.588
118.827
112.422
110.207
95.351
50.104
40.741
40.576
40.499
40.408
40.239
40.074
39.906
39.737
200
180
160
140
120
100
80
60
40
20
ppm
N
CN
COOH
Br

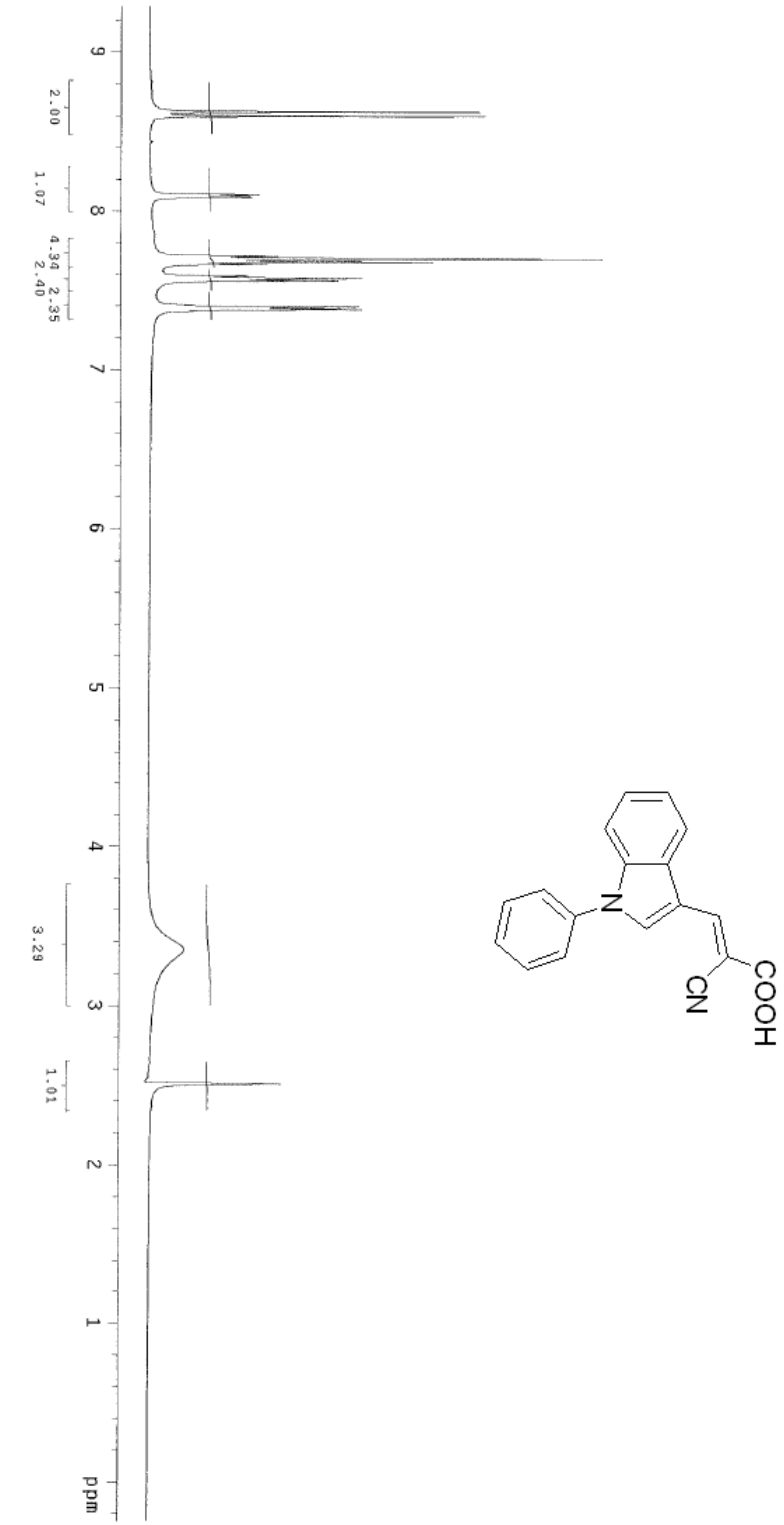
9
8
7
6
5
4
3
2
1
ppm
2.00
1.07
4.34
2.40
2.35
3.29
1.01
N
CN
COOH

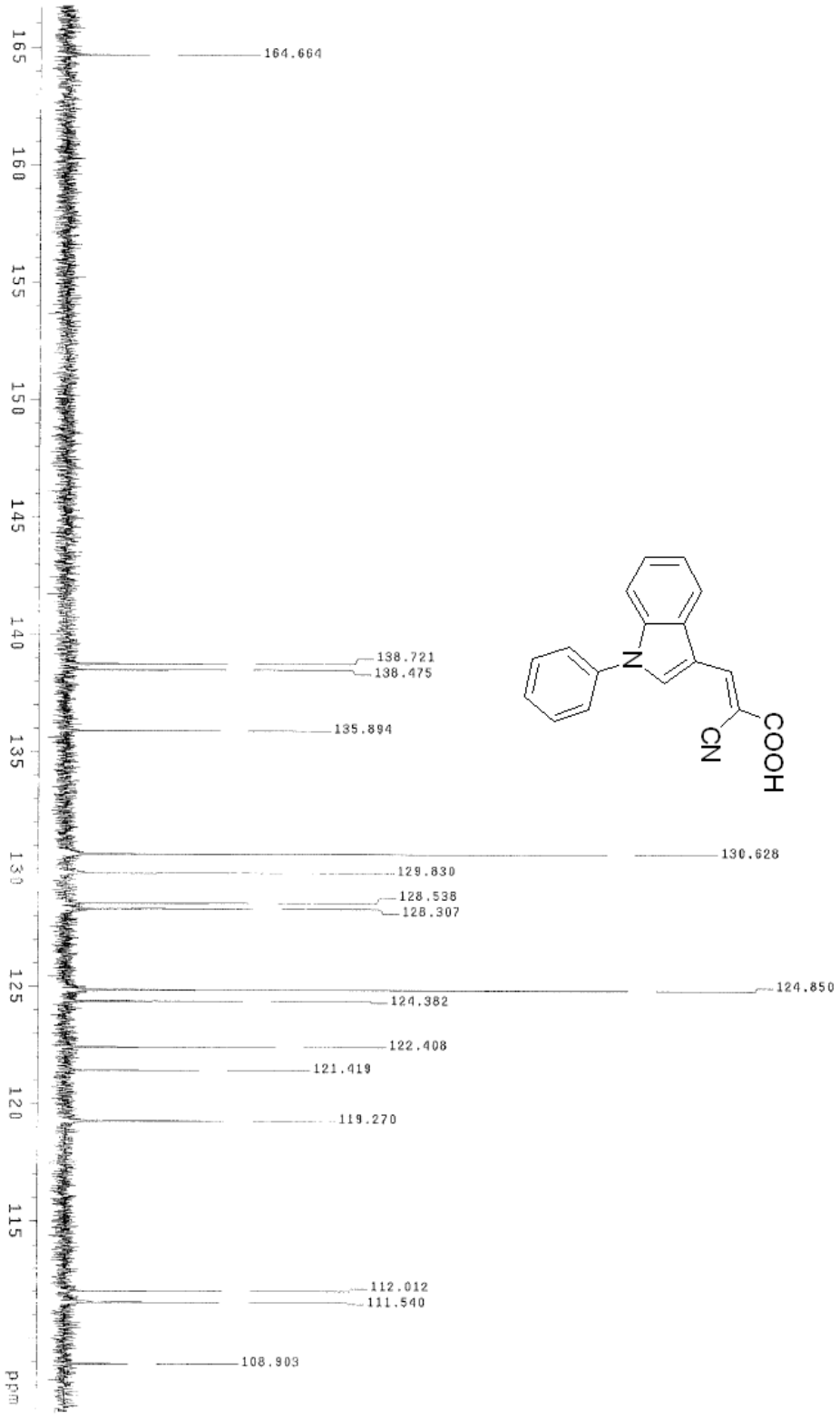
165
160
155
150
145
140
135
130
125
120
115
ppm
164.664
138.721
138.475
135.894
130.628
129.830
128.538
128.307
124.850
124.382
122.408
121.419
119.270
112.012
111.540
108.903
N
CN
COOH

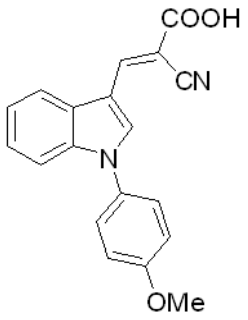
COOH
CN
N
OMe

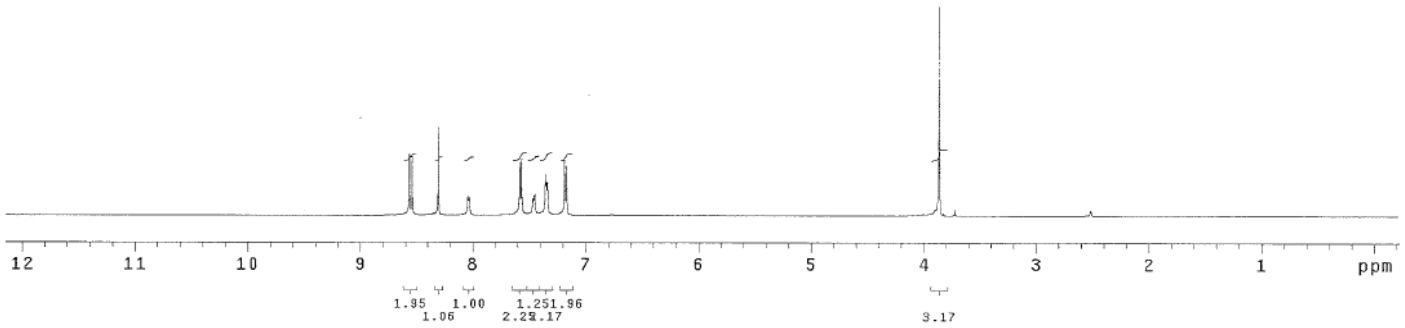
12
11
10
9
8
7
6
5
4
3
2
1
ppm
1.95
1.06
1.00
1.25
2.25
1.96
2.17
3.17

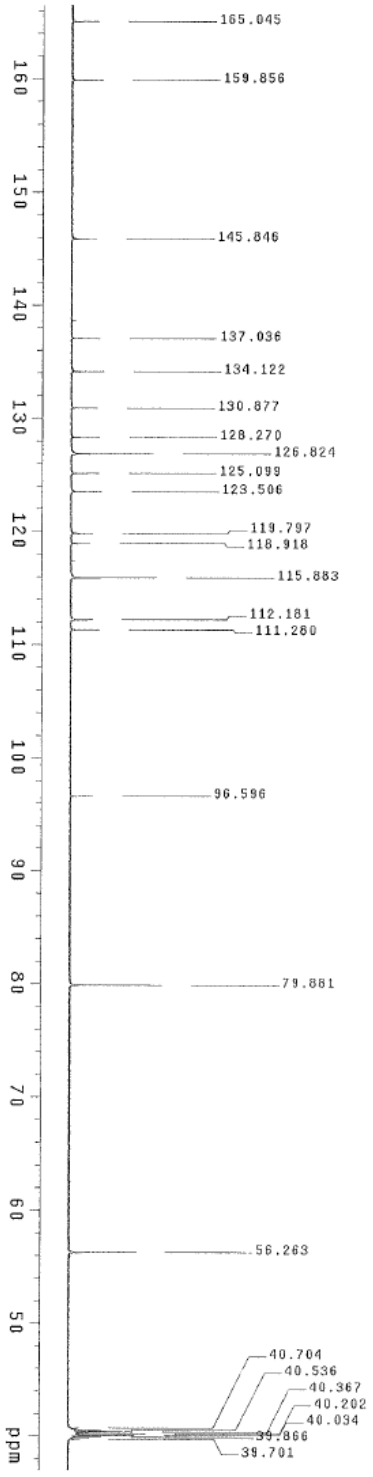
165.045
159.856
145.846
137.036
134.122
130.877
128.270
126.824
125.099
123.506
119.797
118.918
115.883
112.181
111.280
96.596
79.881
56.263
40.704
40.536
40.367
40.202
40.034
39.866
39.701
160
150
140
130
120
110
100
90
80
70
60
50
ppm

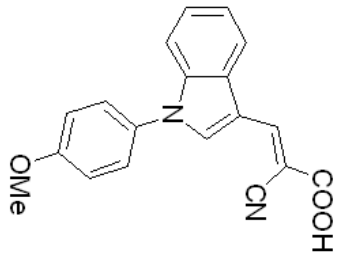
N
OMe
CN
COOH

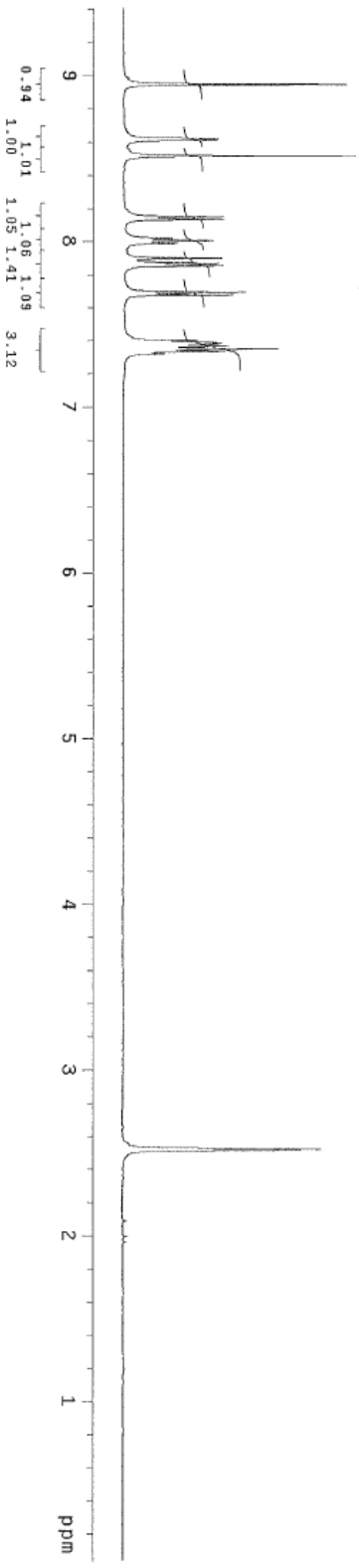
9
8
7
6
5
4
3
2
1
ppm
0.94
1.00
1.01
1.05
1.06
1.41
1.09
3.12

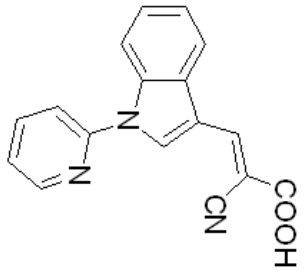
N
N
CN
COOH

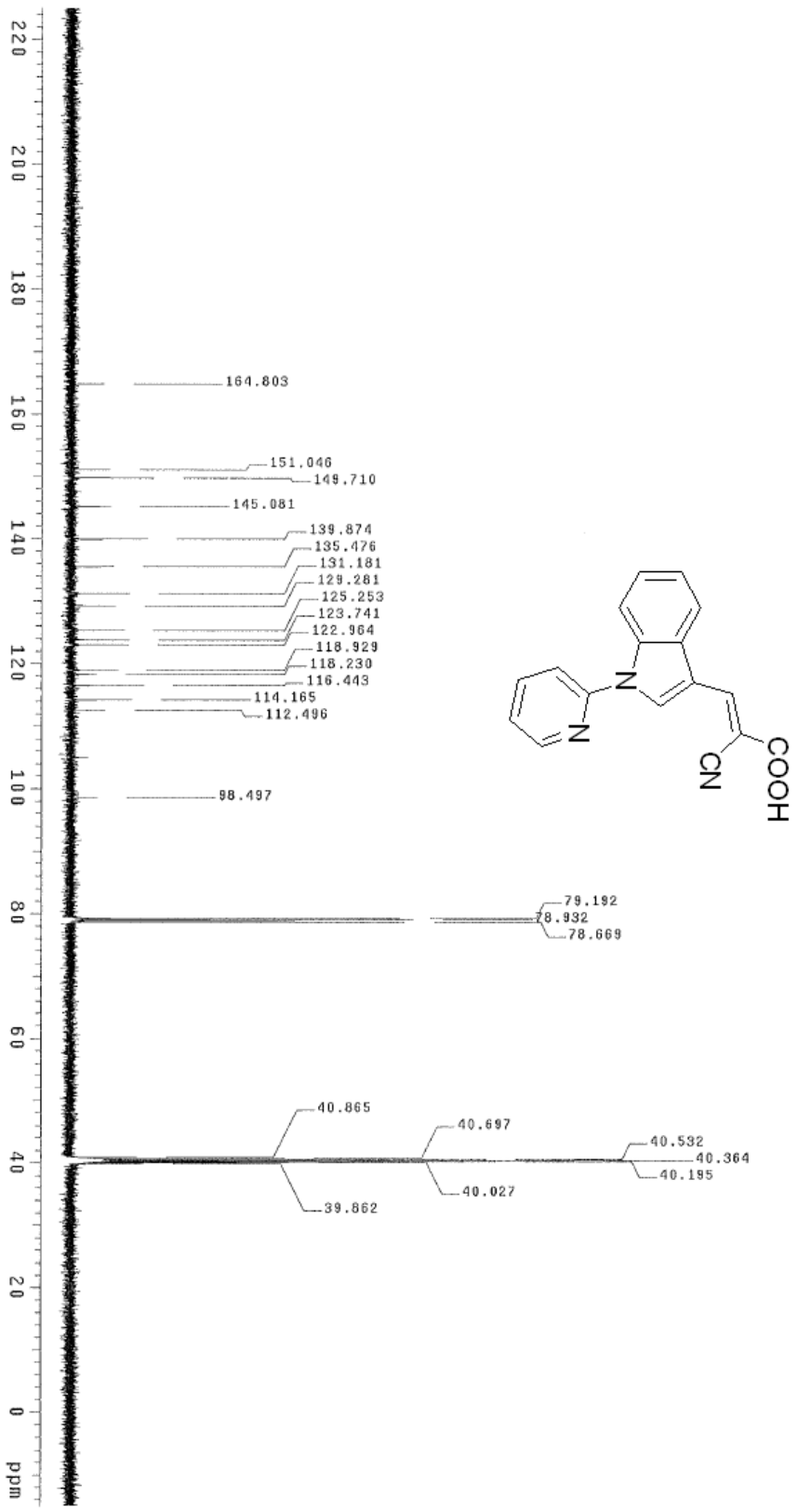
220
200
180
160
140
120
100
80
60
40
20
0
ppm
164.803
151.046
149.710
145.081
139.874
135.476
131.181
129.281
125.253
123.741
122.964
118.929
118.230
116.443
114.165
112.496
98.497
79.192
78.932
78.669
40.865
40.697
40.532
40.364
40.195
40.027
39.862
N
N
CN
COOH

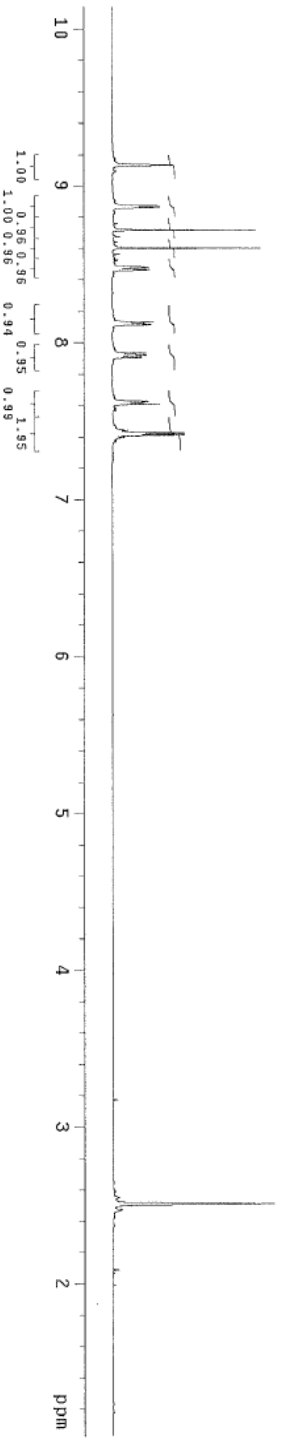
10
9
8
7
6
5
4
3
2
ppm
1.00
1.00
0.96
0.96
0.96
0.94
0.95
0.99
1.95

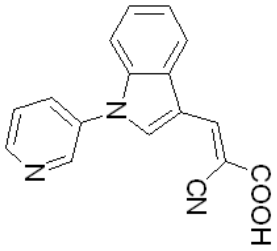
N
N
CN
COOH

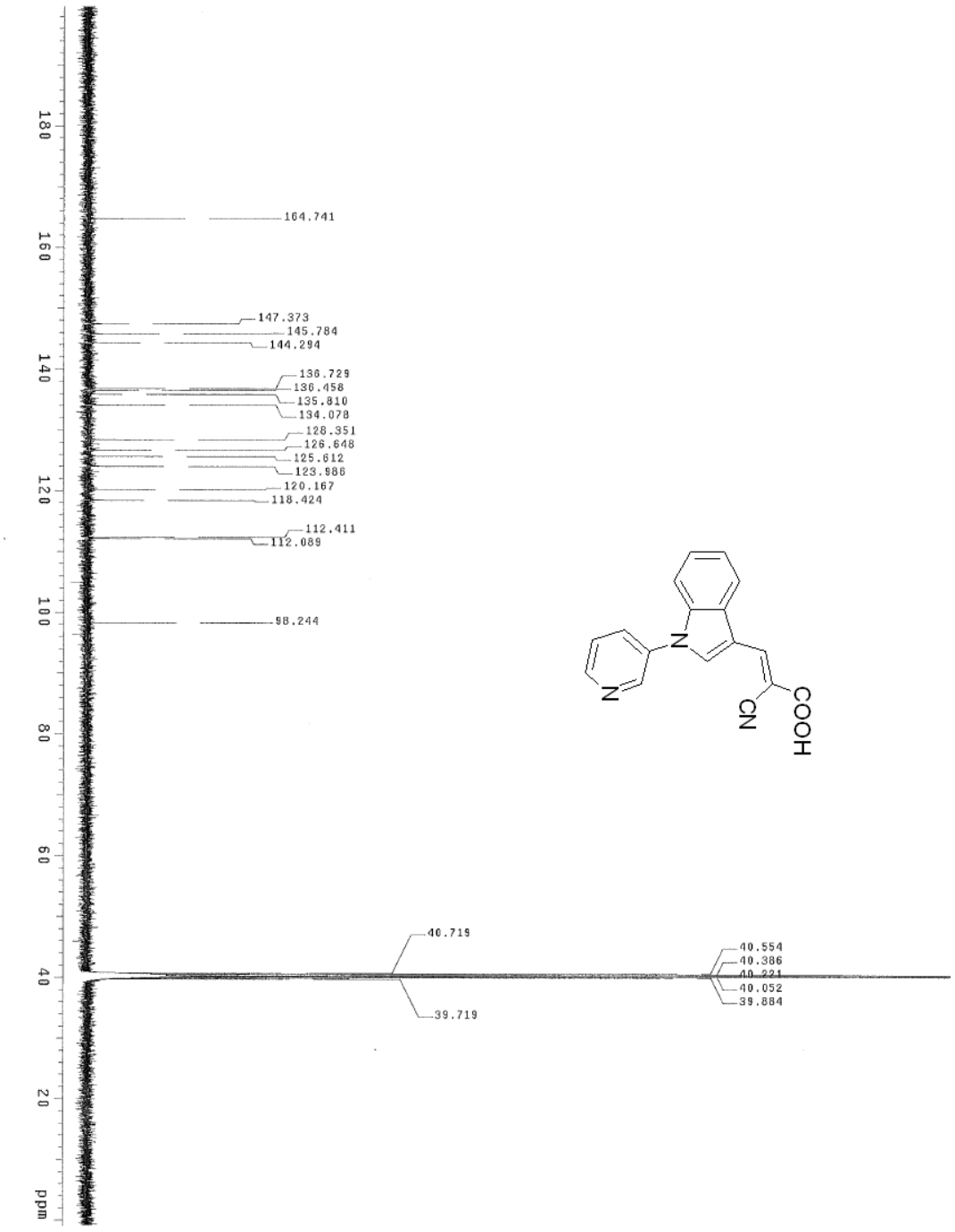
164.741
147.373
145.784
144.294
136.729
136.458
135.810
134.078
128.351
126.648
125.612
123.986
120.167
118.424
112.411
112.089
98.244
40.719
39.719
40.554
40.386
40.221
40.052
39.884
180
160
140
120
100
80
60
40
20
ppm
N
N
CN
COOH

13
12
11
10
9
8
7
6
5
4
3
2
ppm
0.02
1.72
2.00
3.13
2.08
1.08

N
COOH
CN
COOH

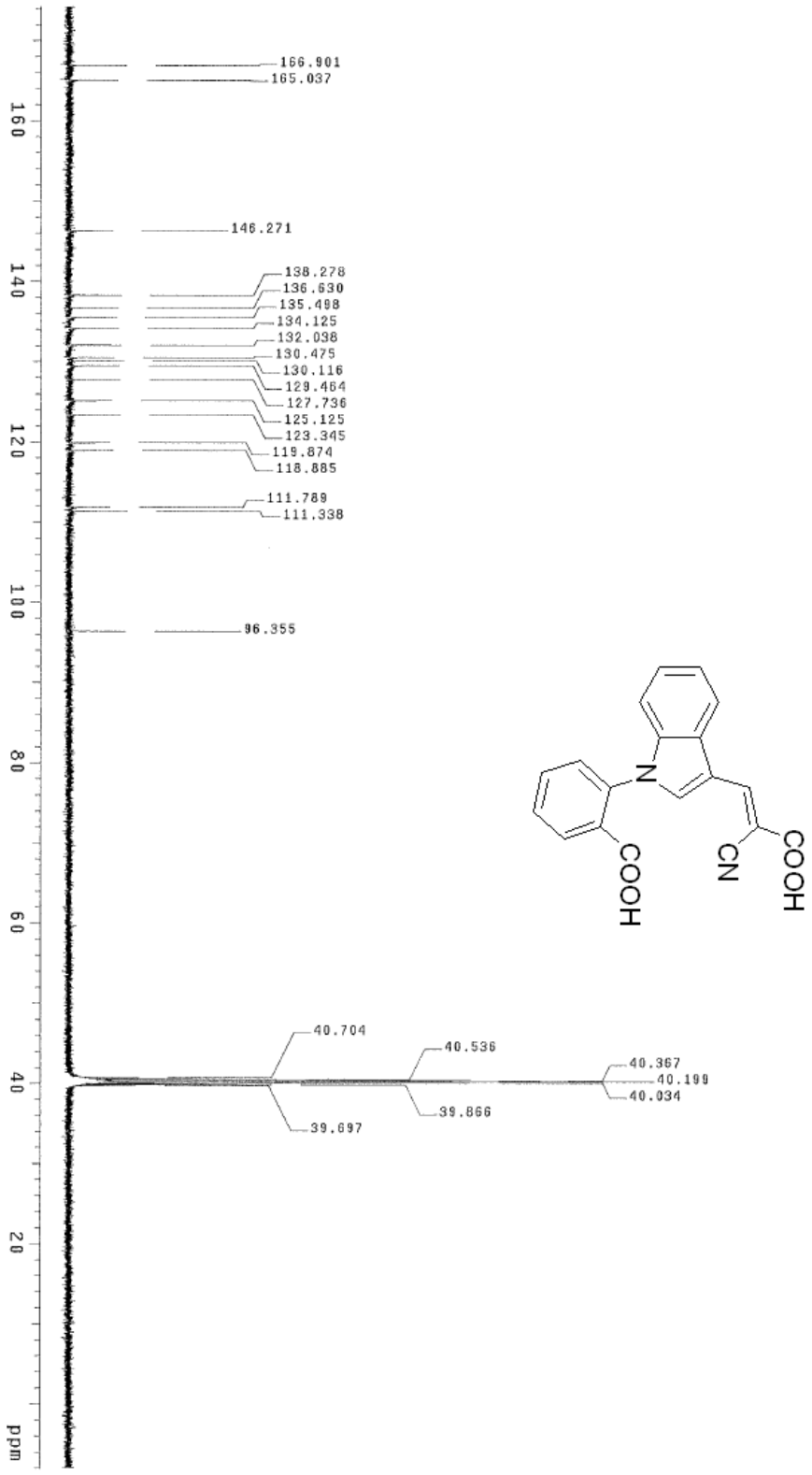
166.901
165.037
146.271
138.278
136.630
135.498
134.125
132.038
130.475
130.116
129.464
127.736
125.125
123.345
119.874
118.885
111.789
111.338
96.355
40.704
40.536
40.367
40.199
40.034
39.866
39.697
160
140
120
100
80
60
40
20
ppm
N
COOH
CN
COOH

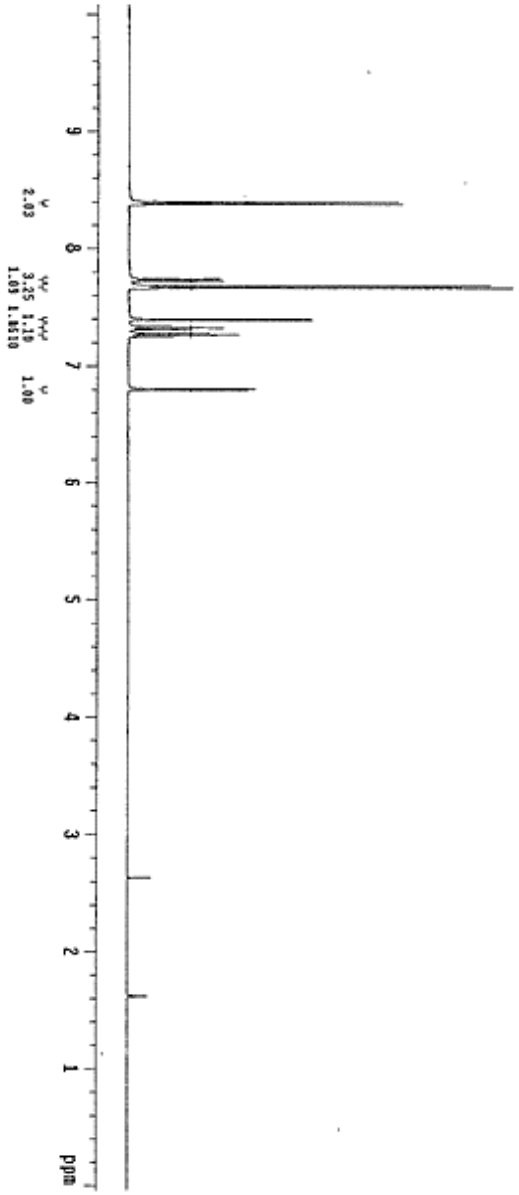
9
8
7
6
5
4
3
2
1
ppm
2.03
3.25
1.19
1.03
1.0810
1.00

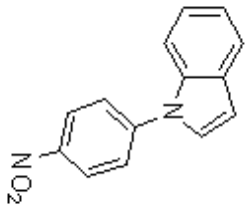
N
NO2

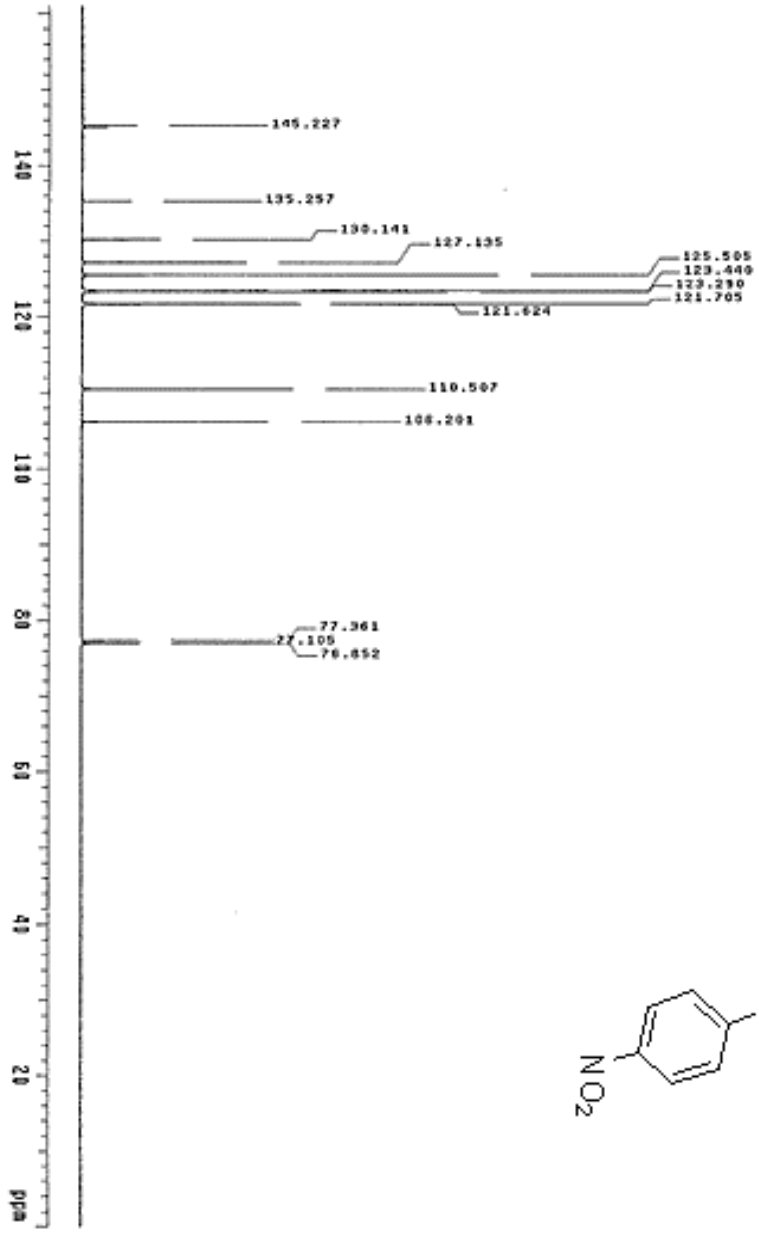
145.227
135.257
130.141
127.135
125.505
123.440
123.230
121.705
121.624
110.507
108.201
77.361
77.105
76.852
140
120
100
80
60
40
20
ppm
N
NO2

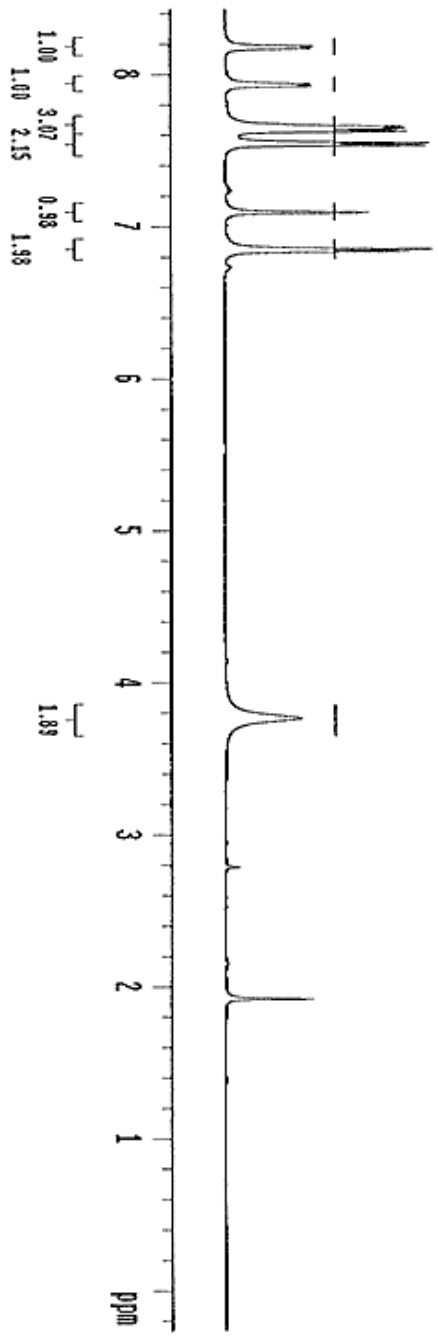
8
7
6
5
4
3
2
1
ppm
1.00
3.07
2.15
0.98
1.93
1.89

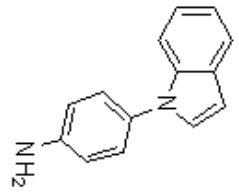
N
NH2

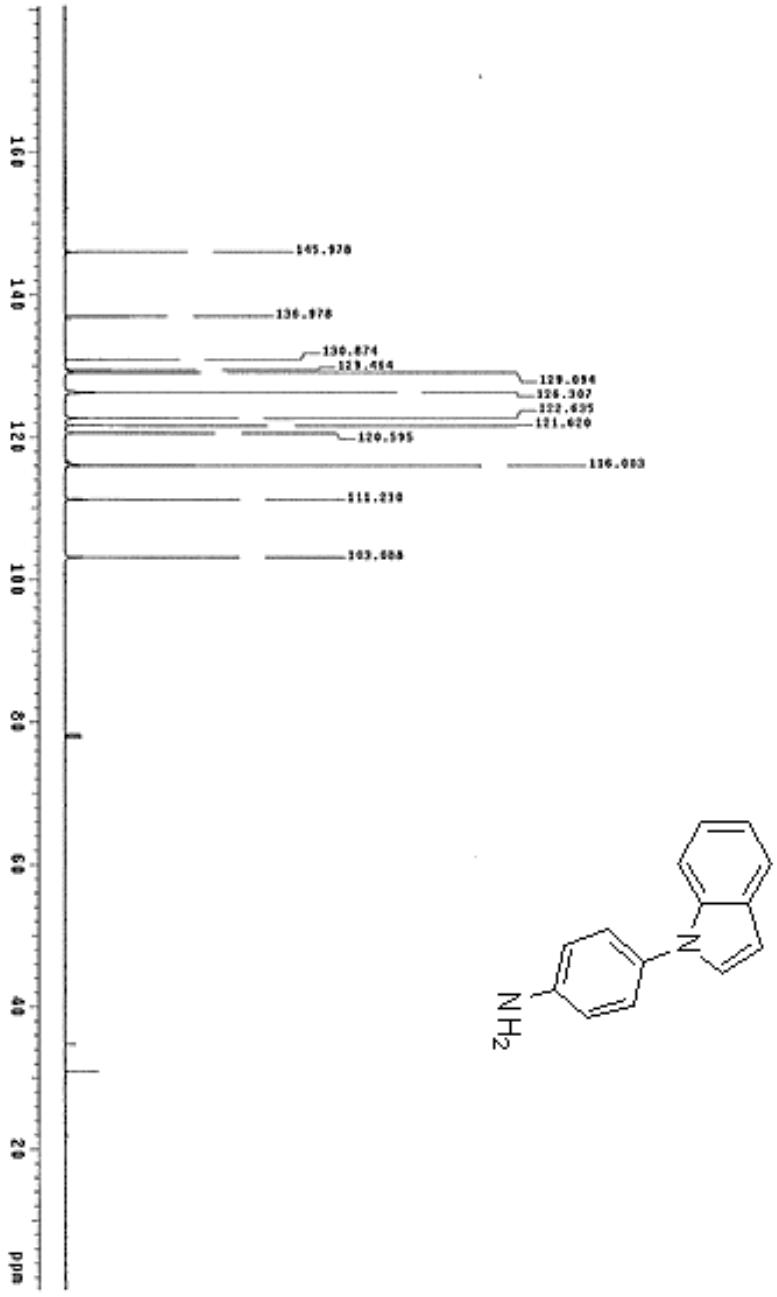
160
140
120
100
80
60
40
20
ppm
145.978
136.978
130.874
129.464
129.054
126.307
122.635
121.620
120.595
116.003
115.210
103.088
N
NH2

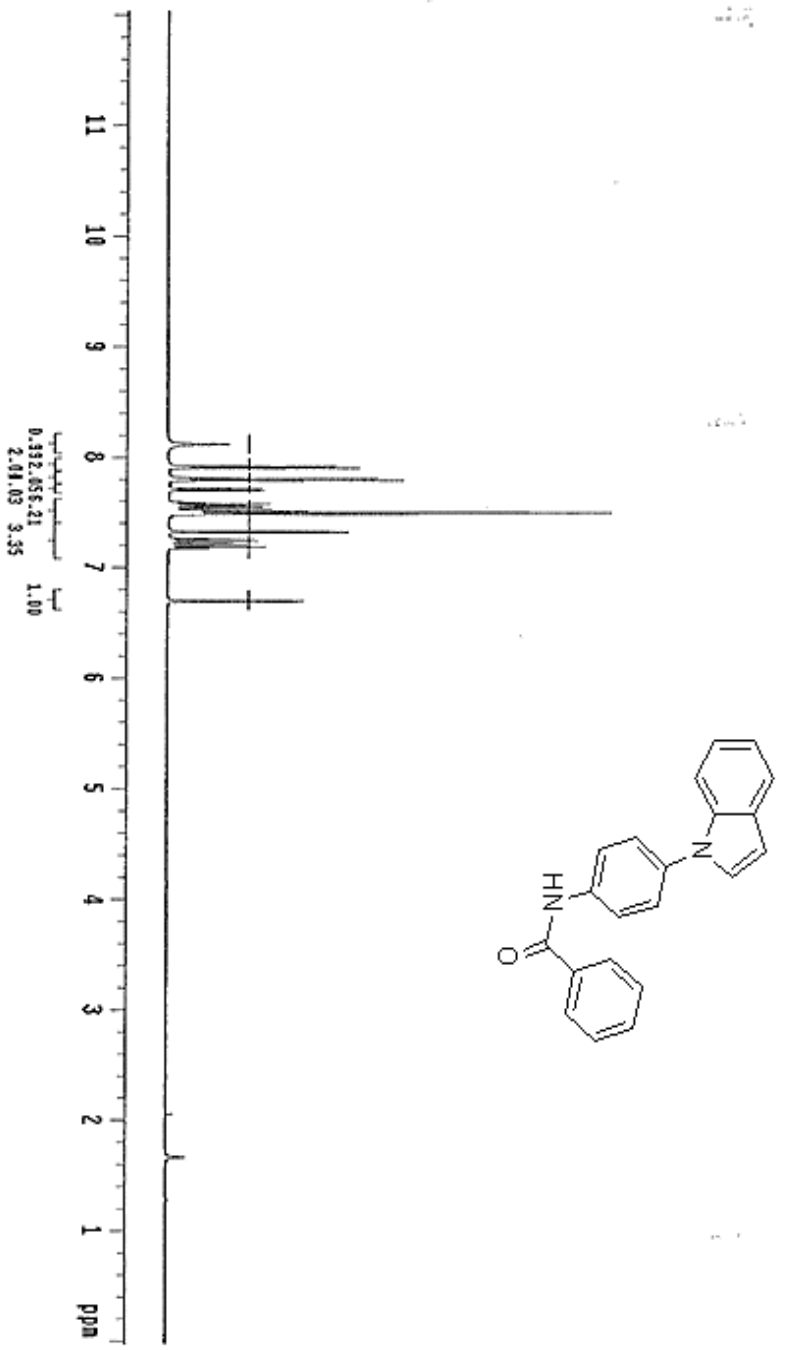
HN
O
N
ppm
1
2
3
4
5
6
7
8
9
10
11

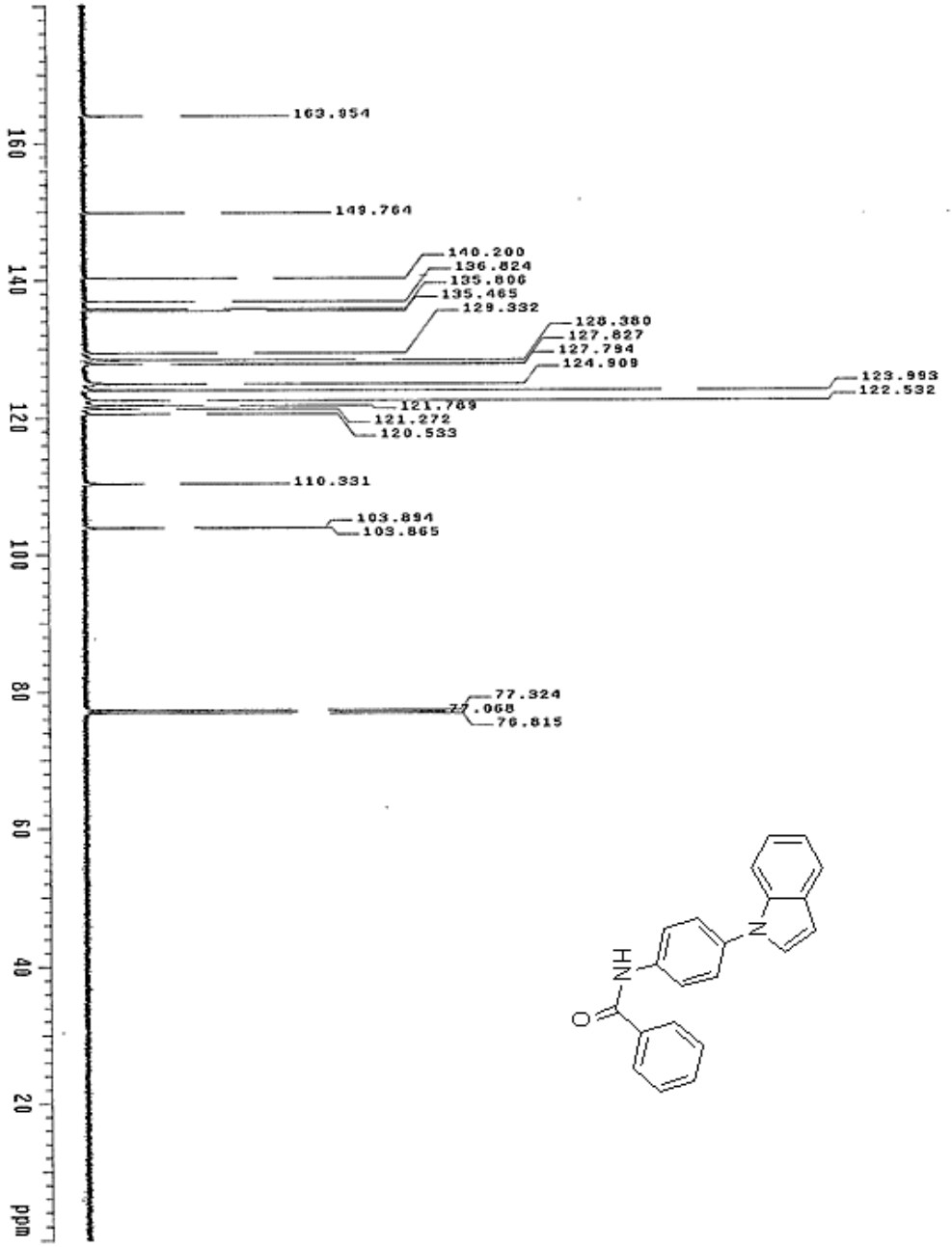
163.954
149.764
140.200
136.824
135.806
135.465
129.332
128.380
127.827
127.784
124.909
123.993
122.532
121.769
121.272
120.533
110.331
103.894
103.865
77.324
77.068
76.815
160
140
120
100
80
60
40
20
ppm
NH
O
N

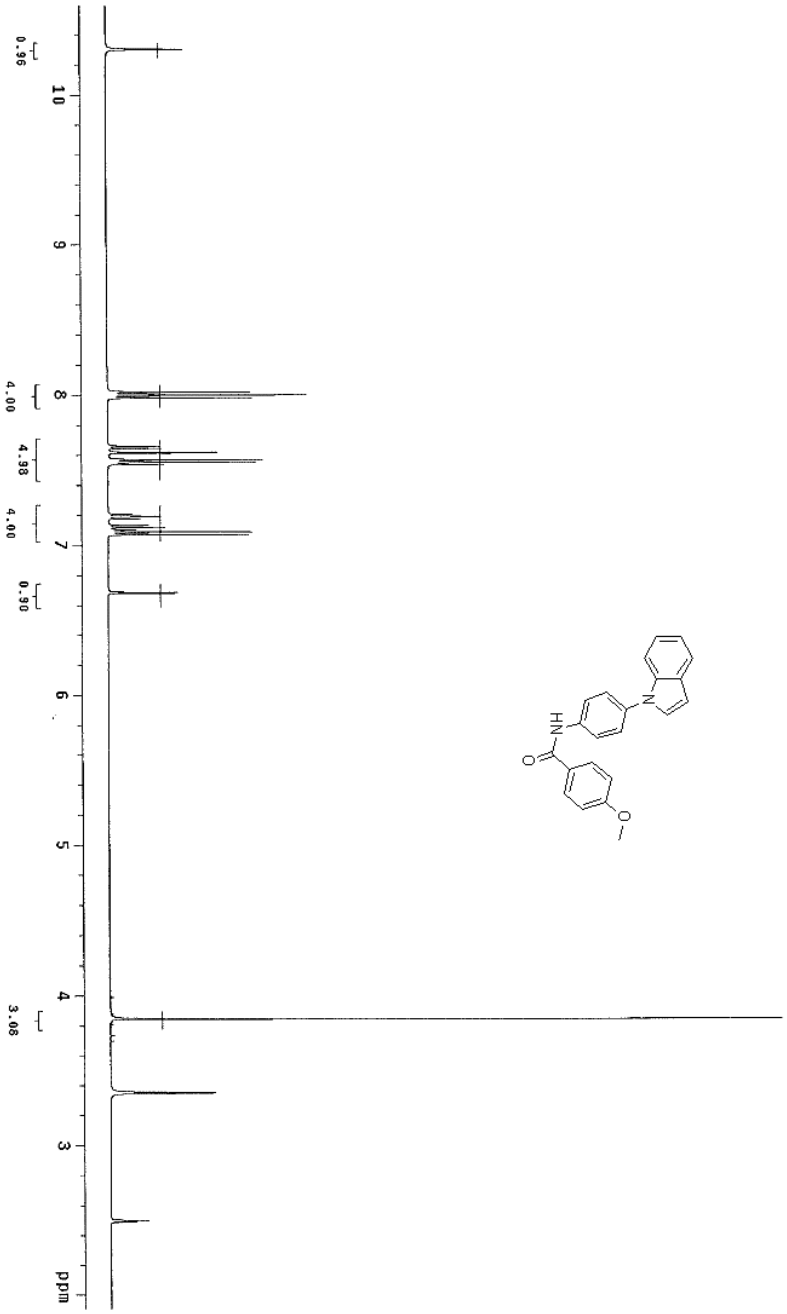
0.96
4.00
4.98
4.00
0.90
3.06
10
9
8
7
6
5
4
3
ppm
HN
O
O

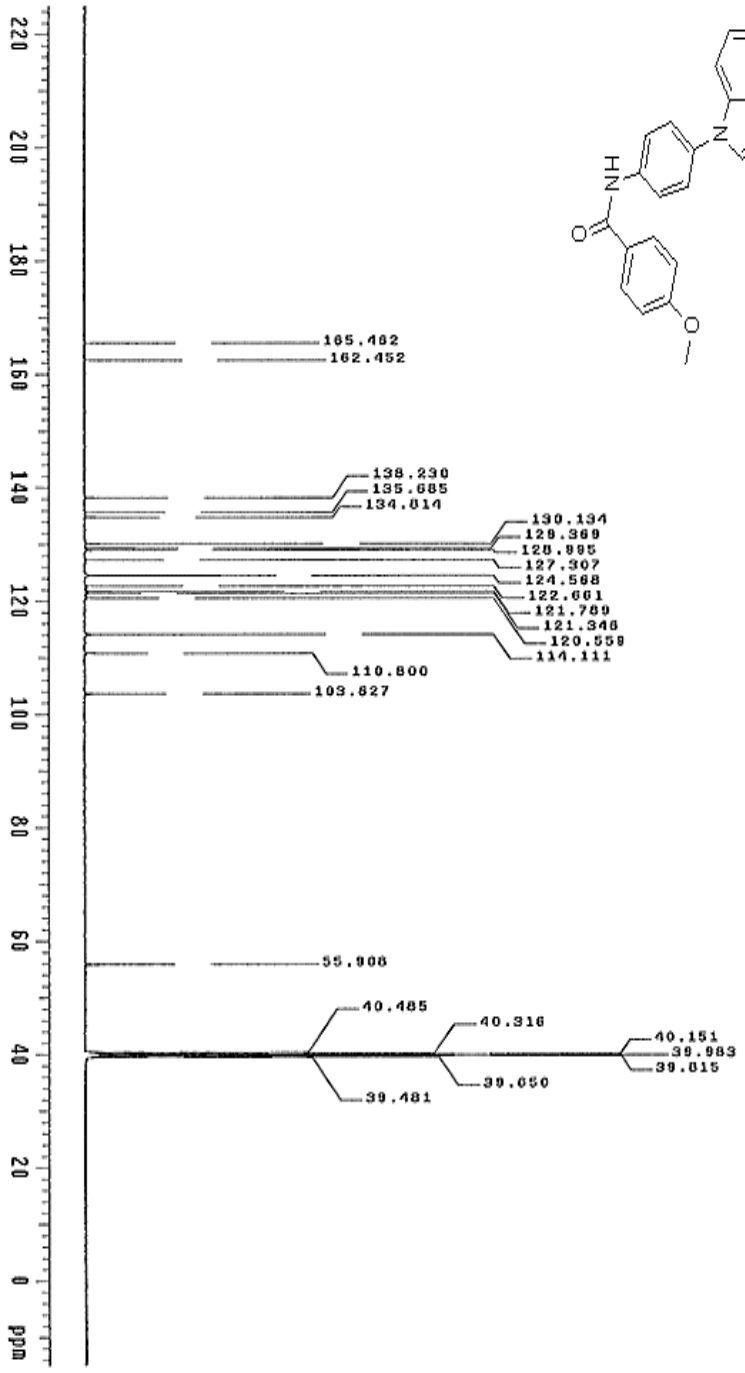
220
200
180
160
140
120
100
80
60
40
20
0
ppm
165.482
162.452
138.230
135.685
134.014
130.134
129.369
128.995
127.307
124.568
122.661
121.789
121.346
120.558
114.111
110.800
103.827
55.908
40.485
40.316
40.151
39.983
39.815
39.650
39.481
HN
N
O
O

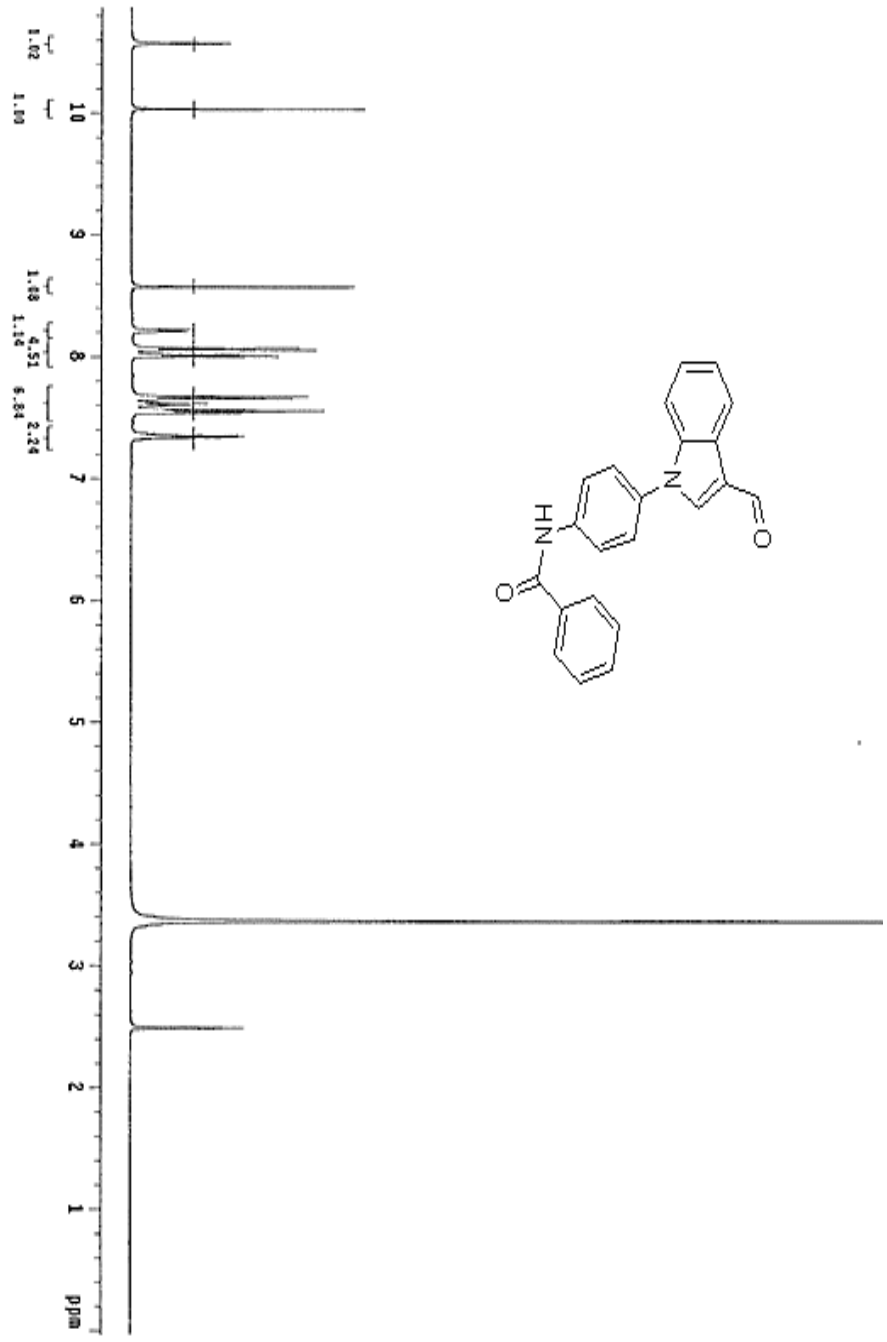
1.02
1.00
1.88
4.51
1.14
6.84
2.24
10
9
8
7
6
5
4
3
2
1
ppm
HN
O
N
O

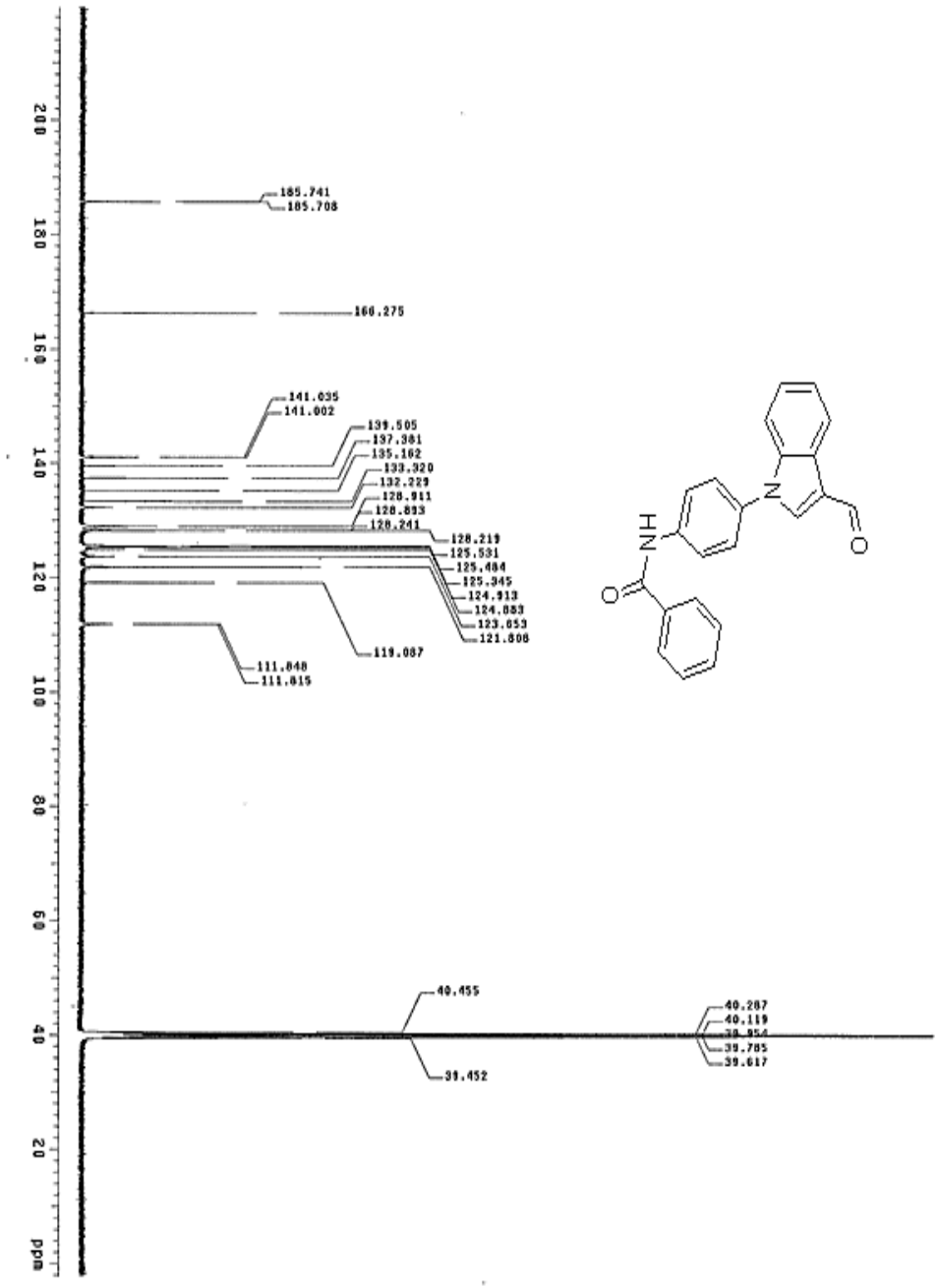
185.741
185.708
160.275
141.035
141.002
139.505
137.381
135.162
133.920
132.229
128.911
128.893
128.241
128.219
125.531
125.484
125.345
124.913
124.883
123.653
121.808
119.087
111.848
111.615
40.455
40.287
40.119
39.785
39.617
39.452
NH
O
N
O
ppm

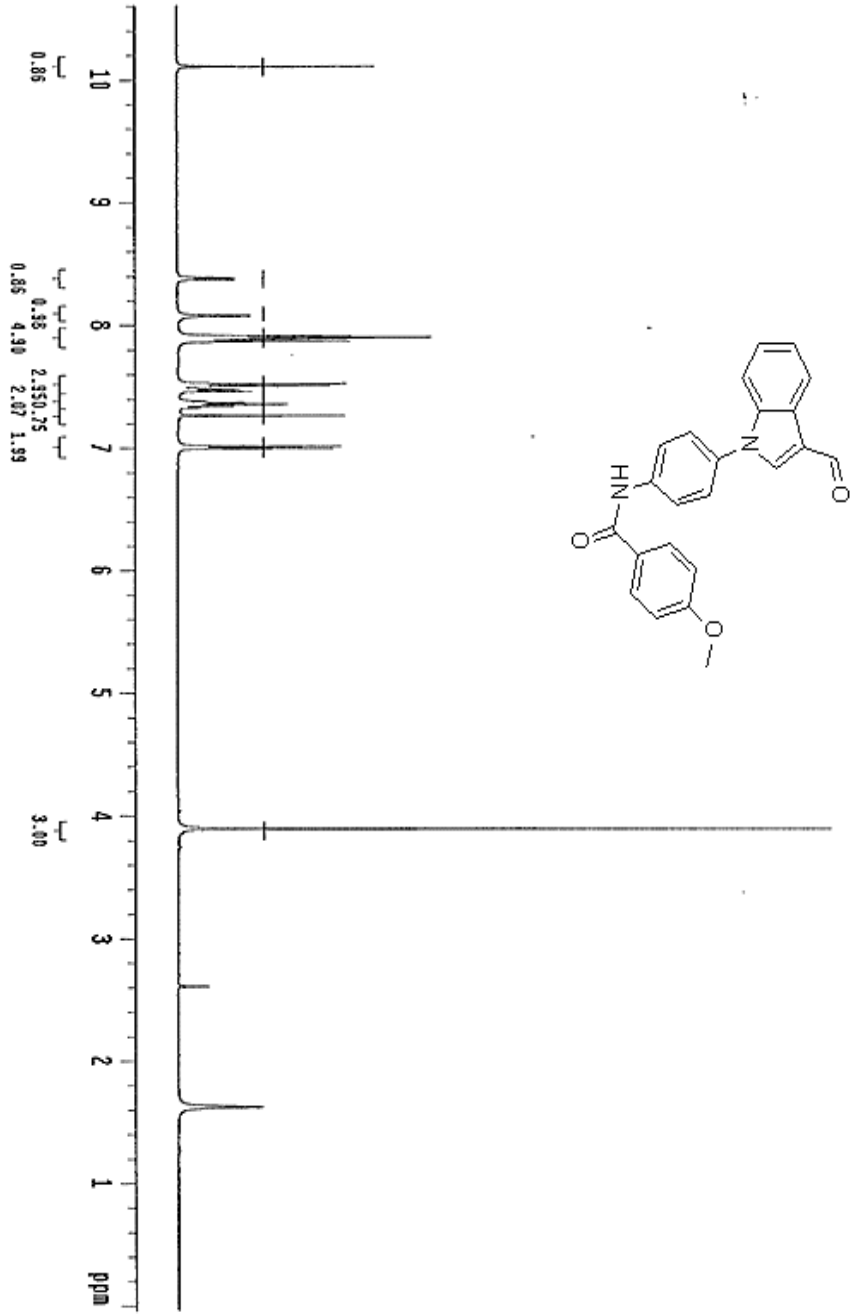
10
9
8
7
6
5
4
3
2
1
ppm
3.00
0.86
0.86 4.90 2.07 1.99 0.95 2.95 0.75

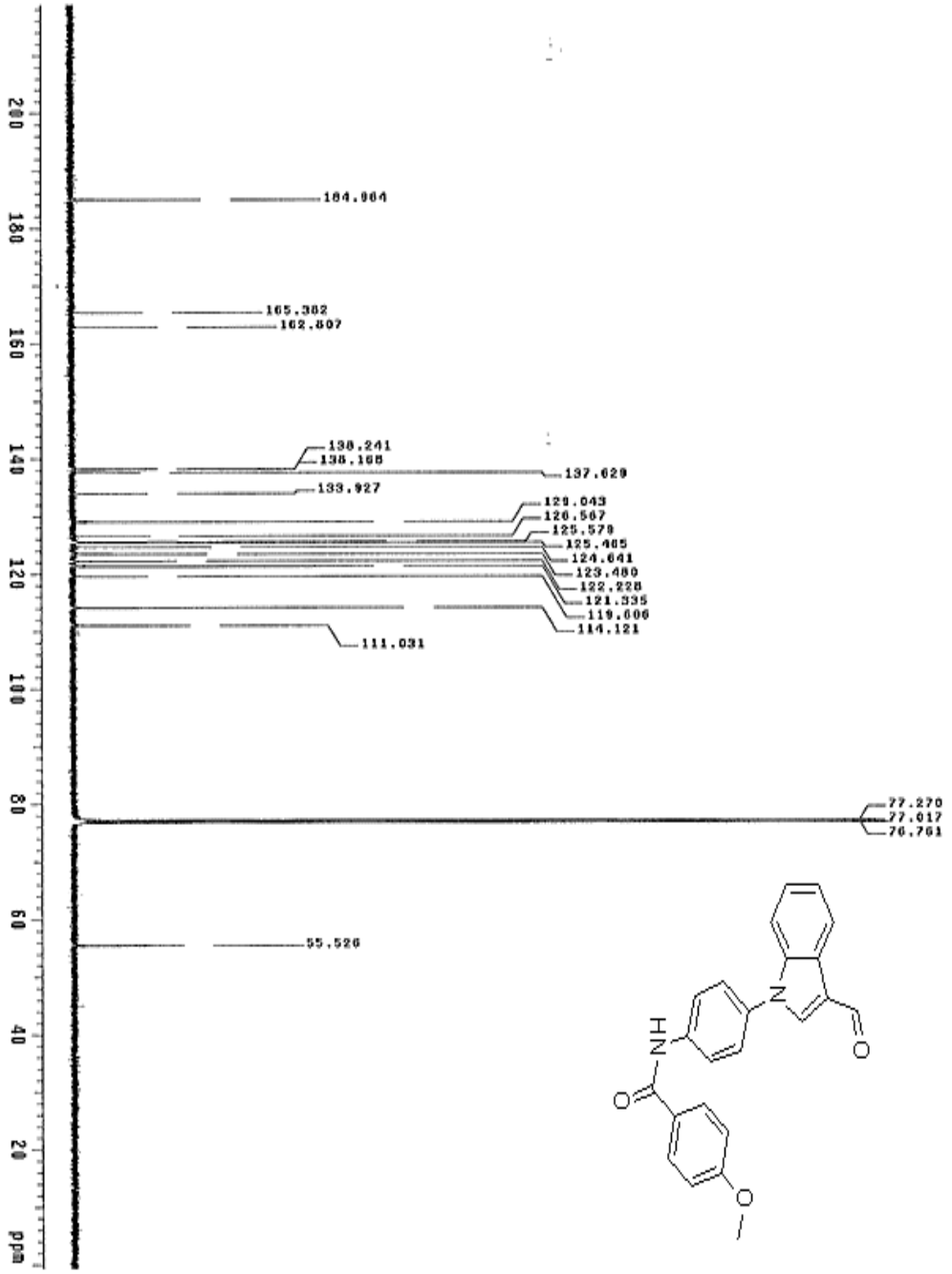
184.064
165.382
162.807
138.241
138.165
137.629
133.927
129.043
126.567
125.579
125.465
124.641
123.480
122.228
121.335
119.606
114.121
111.031
77.270
77.017
76.761
55.526
ppm

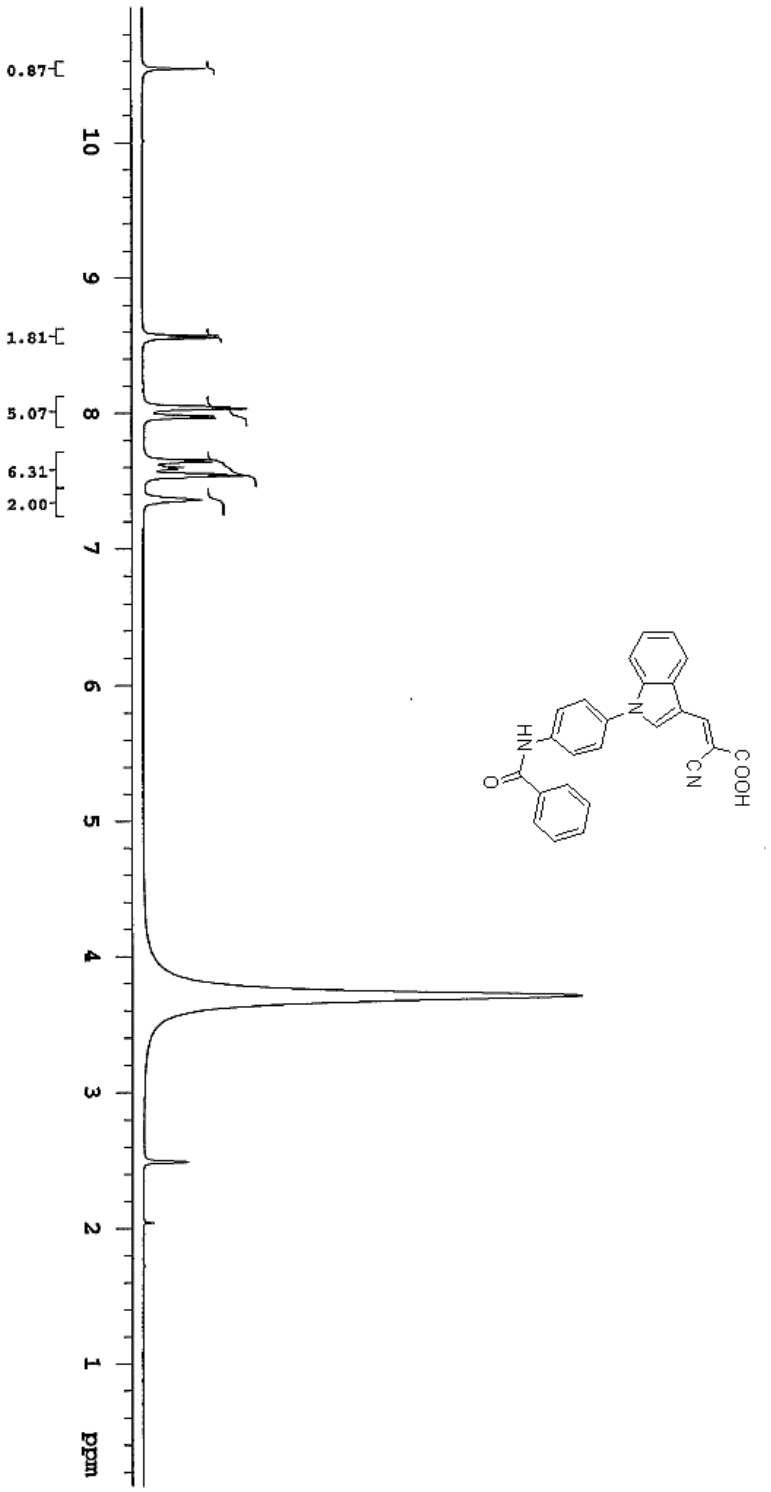
0.87
1.81
5.07
6.31
2.00
10
9
8
7
6
5
4
3
2
1
ppm
HN
O
N
CN
COOH

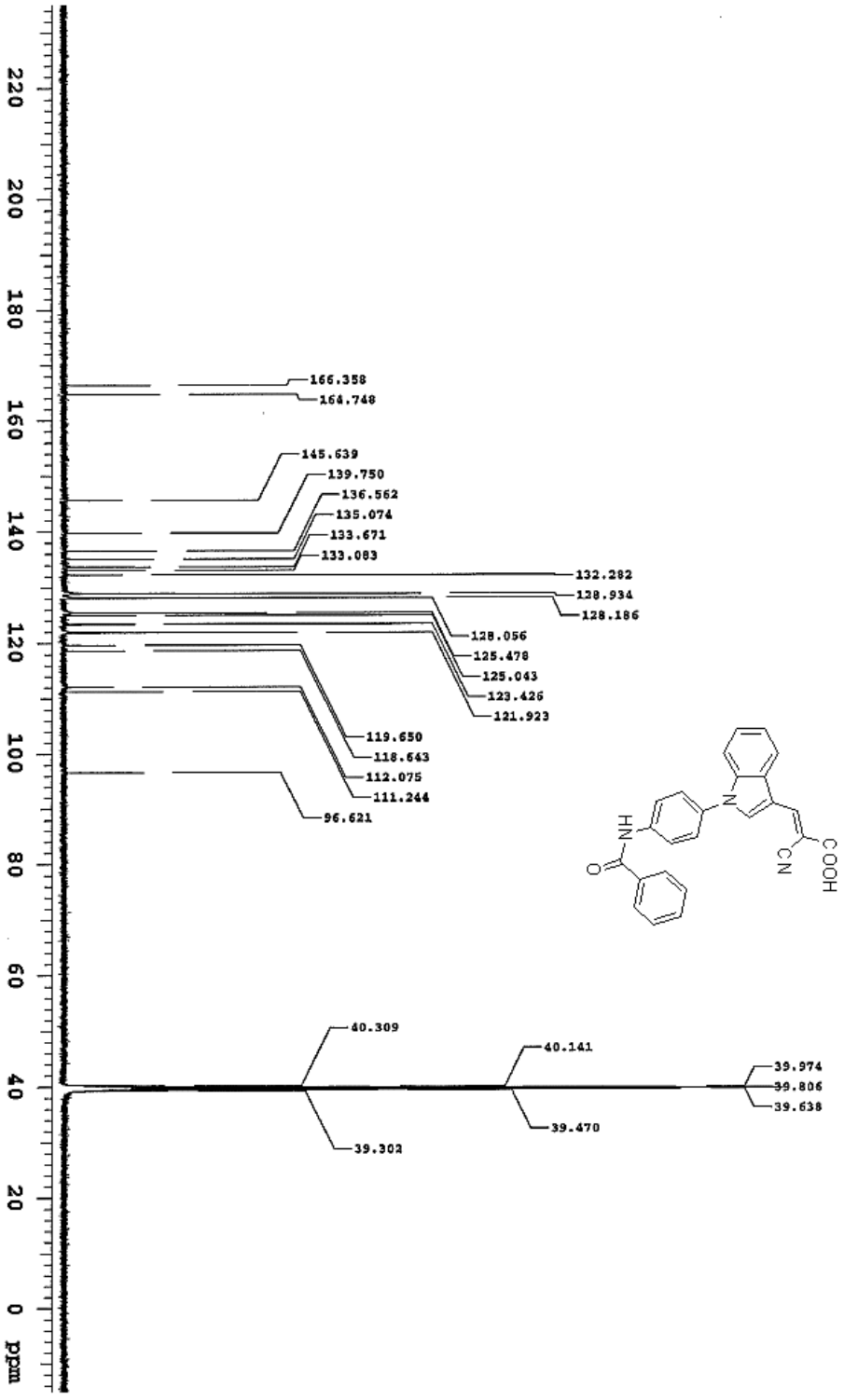
220
200
180
160
140
120
100
80
60
40
20
0
ppm
166.358
164.748
145.639
139.750
136.562
135.074
133.671
133.083
132.282
128.934
128.186
128.056
125.478
125.043
123.426
121.923
119.650
118.643
112.075
111.244
96.621
40.309
40.141
39.974
39.806
39.638
39.470
39.302
HN
O
N
CN
COOH

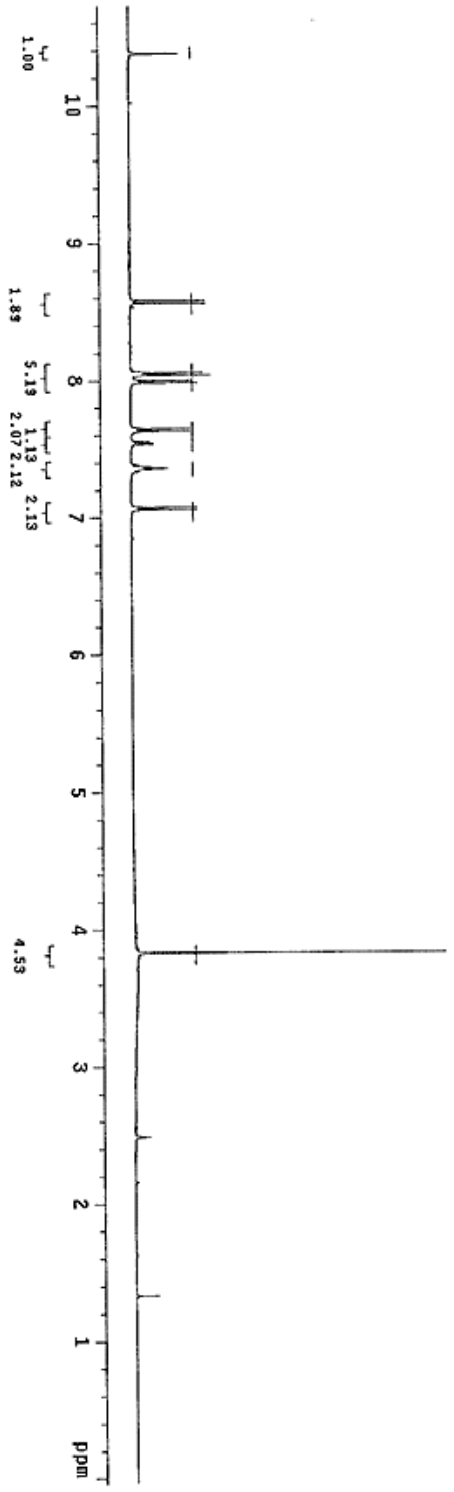
1.00
1.89
5.19
1.13
2.07
2.12
2.13
4.53
10
9
8
7
6
5
4
3
2
1
ppm

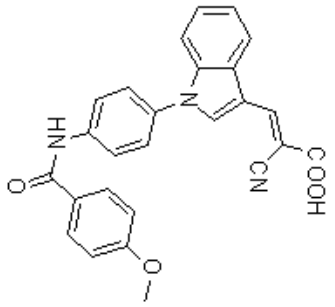
HN
O
N
CN
COOH
O

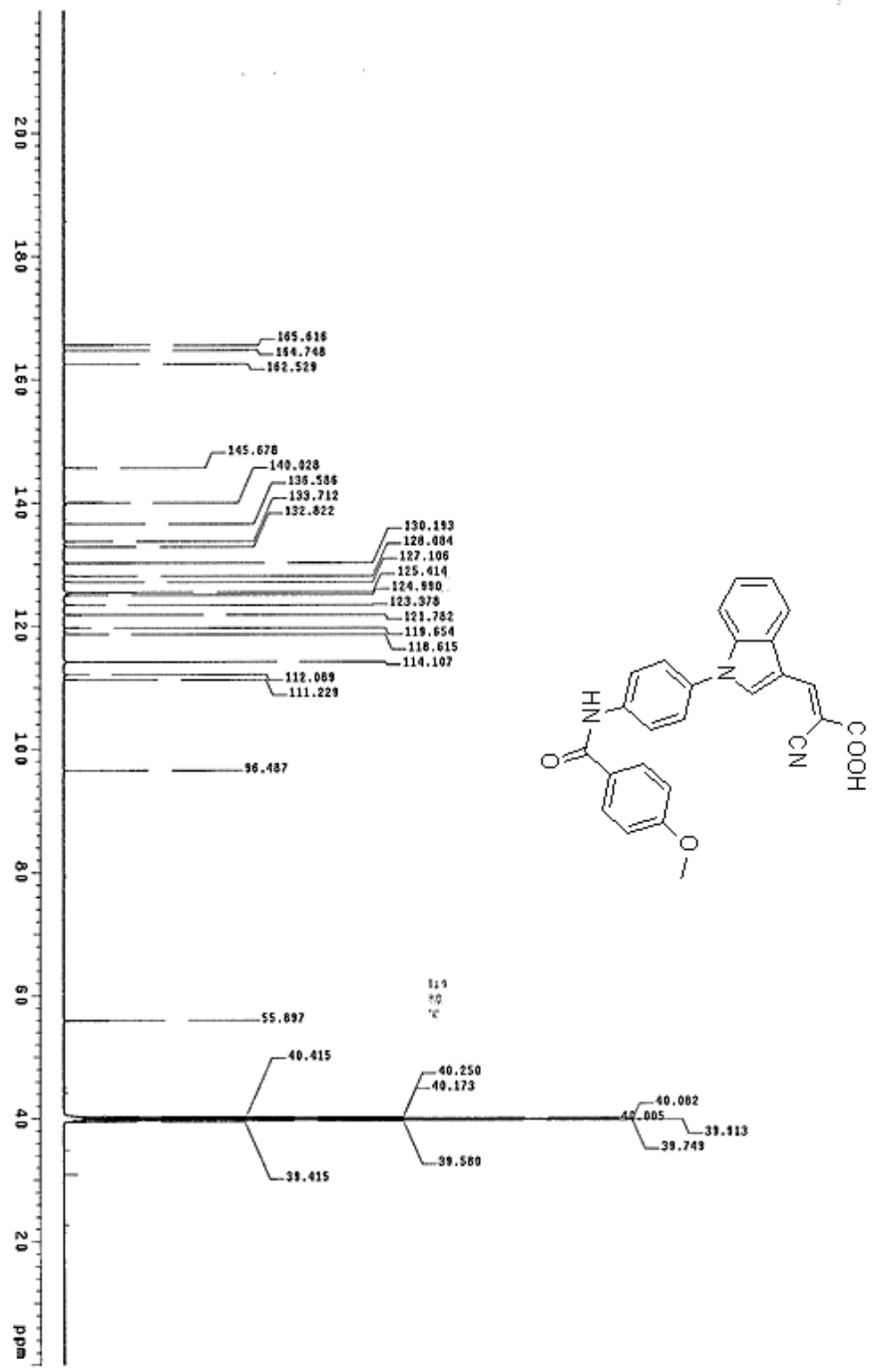
165.616
164.748
162.529
145.678
140.028
136.586
133.712
132.822
130.193
128.084
127.106
125.414
124.980
123.378
121.782
119.654
118.615
114.107
112.089
111.229
96.487
55.897
40.415
40.250
40.173
40.082
40.005
39.913
39.749
39.580
39.415
NH
O
O
CN
COOH
ppm